THE UNIVERSITY OF QUEENSLAND

BACHELOR OF ENGINEERING THESIS

Investigation of Natural Draft Dry Cooling Tower Design and Construction

Student Name: Lachlan A. JEFFERIS

Student Number: 43238190

Course Code: MECH4500

Supervisor: Mr Hugh Russell

Due Date: 28th October 2016

A thesis submitted in partial fulfilment of the requirements of the Bachelor of Engineering degree in Mechanical Engineering

UQ Engineering

Faculty of Engineering, Architecture and Information Technology

ABSTRACT

This thesis investigates the design and construction of natural draft dry cooling towers, with particular emphasis on improving upon an existing design developed by the Queensland Geothermal Energy Centre of Excellence to reduce the total installed costs of cooling towers to make providing cost effective renewable energy solutions to rural and remote communities more viable. Traditionally, cooling towers are not economic for small-scale applications, which makes implementing renewable power plants for localised electricity grid systems costly and impractical compared to non-renewable methods currently being used.

Through review of literature, existing state-of-the-art modular designs were identified, and a potential for improvement was recognised. In accordance with applicable standards, loading such as pretension and wind loads were determined. A comparative study was conducted to validate previous analysis performed on the existing Queensland Geothermal Energy Centre of Excellence Hybrid Cooling Tower, to replicate and ascertain assumptions and boundary conditions. Observations made from the comparative study were used to conduct a benchmark analysis, which was used to develop a benchmark of design and define maximum permissible design values, to be used to compare against alternative designs developed throughout the thesis. Investigation and analysis was conducted on alternative construction methods and structural geometries using both numerical and analytical methods.

Conclusions from analysis present three alternative design solutions, one for an alternative construction method, and two alternative structural geometries. The alternative construction method, the Tilt-Up Tower, eliminates the need for specific cranes for one-off lifts, by implementing a winch and gin pole to erect the structure by tilting it from the ground up. The two alternative structural geometries, designated Alternative A and Alternative B, simplify the geometry of the existing tower by reducing the number of structural members in favour of guy wires that are either anchored externally (Alternative A) or internally (Alternative B).

It is recommended that to reduce construction and cranage costs implement the Tilt-Up Tower, and to reduce construction, manufacturing, and total installed costs implement either Alternative A or Alternative B. Alternative B is the recommended structural geometry alternative because of the minimal installed building footprint compared to Alternative A.

ACKNOWLEDGEMENTS

This thesis would not have been possible with the guidance and support of a number of people, all to whom I extend my most sincere thanks. Foremost, I would like to thank my supervisor, Mr Hugh Russell, for firstly accommodating me and providing me with the opportunity to take on this project, without whom I may not have been able to undertake a project, which I can happily say I have thoroughly enjoyed. I would also like to thank Hugh for his patience, guidance, continuous feedback, and for pushing and challenging me to do my best throughout the year.

I would also like to thank Mr David Stevens, and anyone else within the Queensland Geothermal Energy Centre of Excellence who contributed to the eventuation of this project, and the special efforts made to create a topic specific to my interests, skills and experiences.

I would like to extend a brief thanks to the Head of the School of Mining and Mechanical Engineering Professor David Mee, and any other staff, academia, or special guest that contributed to the course under which this thesis was conducted, MECH4500, for all the efforts and logistics undertaken to give students the tools to succeed and develop professionally as engineers.

To family and friends who were pivotal in helping me throughout my degree, I could not be any more grateful, particularly in this final year, for the tireless support and sacrifice you have made to make sure I have gotten where I am. Finally yet importantly I would like to express my heartfelt gratitude to my girlfriend Emma who without I may not have made it this far. For her unwavering support throughout a challenging and trying four years of my degree, for understanding the stress and sometimes frustration I was experiencing, and for pushing me to keep going when I thought I had had enough.

CONTENTS

LIST OF FIGURES

LIST OF TABLES

“People of mediocre ability sometimes achieve outstanding success because they don’t know when to quit. Most men succeed because they are determined to.”

– George E. Allen

1 INTRODUCTION

Cooling towers are commonly used in large power plants for cooling process fluids. However, they are not economic on a small scale because of the specialist and innovative structural designs and construction techniques required. Natural Draft Dry Cooling Towers (NDDCT's) are a cost effective means of cooling for use in renewable thermoelectric power plants due to the lower consumption of water as compared to wet cooling, and auxiliary power is not required for the operation of drafting fans.

1.1 Background

Rural electrification is the process of providing electrical power to rural and remote areas. Rural and remote areas, or communities of low socioeconomic status generally do not have access to electricity, whether it be from a national or local grid system [1]. Where local or isolated grid networks are used, which use technologies that typically are non-renewable, such as diesel generators, are costly to operate, maintain, have high fuel import costs, and are harsh on the environment. Therefore, such areas and communities have the greatest opportunity to make the most of renewable energies for electricity generation. However, any electricity generation method, renewable or not, needs to be cost effective given the lower power demand associated with smaller populations.

In areas that have an abundance of natural renewable energy sources, like thermal energy sources such as solar or geothermal, can harness this energy by the use of thermoelectric power generation. Thermoelectric power plants use thermal energy to heat a working fluid, typically water, to generate steam to power electricity producing turbines. Power cycles used in thermoelectric power plants require some type of cooling, to dissipate waste heat produced by the plant to allow efficient operation. A common method of cooling is with cooling towers, as shown in Figure 1.1.

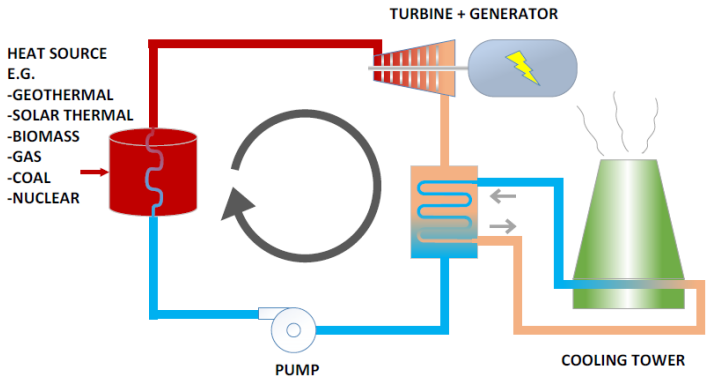

Figure 1.1: Schematic of Thermoelectric Power Plant [2]

Cooling towers are heat rejection devices used in thermoelectric power plants to cool the working fluid, and dissipate waste heat using different methods, which include:

- Wet cooling, which works by principles of evaporative cooling versus;
- Dry cooling, which operates on convective heat transfer through ambient air.
- Mechanical drafted cooling, which uses powered fans to force or induce air flow versus;
- Natural draft cooling, which relies exclusively on air flow and buoyancy effects of the specifically designed structures.

Traditionally, cooling towers are not economically feasible on smaller scales, given their generally large design and construction, which is needed to optimise cooling efficiency.

The Queensland Geothermal Energy Centre of Excellence (QGECE) constructed a state of the art hybrid cooling tower at a research facility at the UQ Gatton campus. The cooling tower is state-of-the-art due to its modular polymer-steel construction, and minimal water consumption.

1.2 Aims & Objectives

The aim of this thesis is to build upon the existing QGECE Hybrid Cooling Tower, focusing on its structural design by:

- Validating existing work and analysis to develop a benchmark of design.
- Investigating alternative construction methods to reduce construction costs.
- Investigating alternative structural geometries to reduce total installed costs.

The outcome of successfully completing these objectives would be the proposal of alternative, improved cooling tower designs that have reduced construction and manufacturing costs, cranage, and consequently a reduced total installed cost per cooling tower. Reducing total installed costs will subsequently meet the need of providing cost effective renewable energy solutions to rural and remote communities.

1.3 Scope

The extent of this thesis shall be limited to the structural design of cooling towers, excluding thermodynamic design, heat transfer methods, and air flow mechanics of cooling towers. The design, failure, and structural analysis of tensile membrane structures being used as cooling tower shells shall also be excluded. Conclusions made on costs shall be implied, as specific cost analysis will not be conducted. Cooling tower structures being analysed in this thesis shall be limited to modular steel designs, and the framework associated, such as the one developed by the QGECE.

2 LITERATURE REVIEW

This chapter aims to evaluate state-of-the-art designs for the structural design of cooling towers. In doing so, the need for an improved design will be substantiated. Techniques and standards, which will be relevant to this project, will also be presented and reviewed. Additionally, the application of wind loading to various structures will be critically investigated to develop a methodology, which will present the way in which improved designs shall be analysed.

2.1 Existing Cooling Tower Design

The QGECE has previously developed a state-of-the-art cooling tower design which aimed to reduce water consumption and the cost of generating electricity in regional parts of Australia [3]. The tower was of a polymer-steel construction, which could flexibly provide either dry, wet, or hybrid cooling. The cooling tower was innovative for its ease of deployment to remote areas, thanks in part to its modular construction, which presented a far cheaper, smaller alternative to traditional cooling towers. The QGECE Hybrid Cooling tower (Figure 2.1) was deployed at a research facility located at the UQ Gatton Campus in regional South East Queensland.

Figure 2.1: QGECE Hybrid Cooling Tower [2]

The sheer size and scale of the tower, which stands 20 m tall, and 12 m in diameter, presents a limitation on the minimum sized crane required to lift the large amounts of structural steel framework into position [4], contributing to increased construction costs. At present, it is stated that the modular design contributes up to a 40% reduction in construction costs [2] when compared to traditional reinforced concrete cooling towers, however this figure could be increased if the design was to be revisited, and optimised.

Shaharuddin [5] conducted a structural analysis on the existing QGECE Hybrid Cooling Tower, which intended to determine the structural integrity of the tower under wind loading in the area where it was constructed. The study concluded that the QGECE Hybrid Cooling Tower would be safe from failure under maximum loading conditions. Ambiguity with the methodology raises questions as to how loads were applied when conducting finite element (FE) simulations.

For example, the determination and application of loads due to pretension of the polymer membrane prior to wind loading was not factored. Additionally, wind loading was considered solely as a horizontal load acting on the tower structure. However, natural tensile stretching of the membrane due to horizontal wind loading will occur, where this stretching will be acting to pull inward on the windward facing side of the tower in relation to the membranes anchorage. This pulling will transmit both a horizontal and vertical load to the top and bottom support structure of the tower. Furthermore, the calculated wind pressure was applied directly to the tower structure, where the correct application of these loads according to the shape of the structure was not considered.

The design of the QGECE Hybrid Cooling Tower itself consisted of two 12 m diameter 323.9 × 9.5 mm grade C350 CHS structural steel ring beams spaced 15 m apart, located 5 m above ground level. The ring beams were supported by four pairs of vertical 273.1 × 6.4 mm C350 CHS structural steel columns, arranged to maintain maximum tower stability. A Mehler PVC [6] membrane, attached to the top and bottom ring beams gave the cooling tower its hyperboloid shell. The analysis conducted by Shaharuddin did not include the bottom ring beam, which could have influenced the results.

2.2 Wind Loads on Cooling Towers

Cooling towers are typically tall structures, ranging from 20 m to 200 m, which presents issues to engineers due to design problems faced by geometry complexities, and wind loading failures. Aside from seismic loading, wind loading is the primary case of loading to affect cooling tower design. There have been some historically spectacular failures, such as the 1965 Ferrybridge tower collapses which were said to have occurred due to an underestimation of the wind loading in the initial design [7]. This highlights the importance of wind load estimation in cooling tower design. Murali et al [8] conducted a study of two cooling towers of 122 m and 200 m in height. The study analysed wind loads on the cooling towers using ANSYS finite element analysis (FEA) software, and assumed fixed supports at the base of the cooling towers. The wind loads were calculated by using circumferentially distributed wind pressure coefficients using Bureau of India Standards. Figure 2.2 shows the circumferential pressure distribution on cooling towers as per Indian Standards. Another study conducted by Gaikwad et al [9] on the effect of wind loading on analysis of natural draft hyperbolic cooling towers, supported by V-shape columns, showed that the circumferential net pressure distribution took on the same characteristics as shown by Murali et al. Furthermore, in the study conducted by Gaikwad et al, it was concluded that the response of cooling towers is governed by both vertical and circumferential wind distribution. These were attributed to quasi-static wind loading which considers the wind

velocity pressure at the towers effective height, an exposure factor that establishes a vertical profile of wind speed, and a coefficient of circumferential wind pressure distribution. Additionally, results of FE analysis showed that circumferential tower membrane stresses were greatest at the maximum height of the tower in consideration. This may be accredited to the loading applied, where dead loading, wind loading, seismic loading, and thermal loading were all considered. Vertical stresses were found to be greatest near the throat.

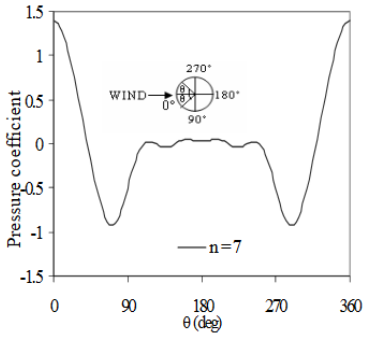

Figure 2.2: Circumferential Pressure Distribution on Cooling Towers [8]

The QGECE Hybrid Cooling Tower employs a hyperboloid shape that has equal diameter at the base and top of the tower, as shown by Figure 2.3.

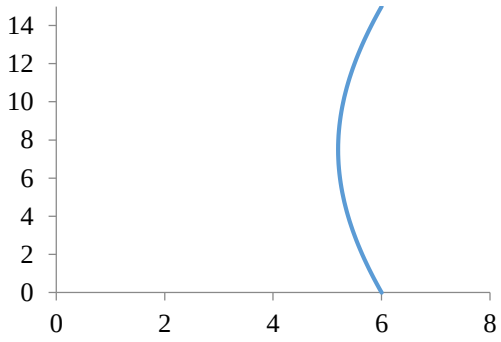

Figure 2.3: QGECE Hyperboloid Shape

The shape of the QGECE hyperboloid shows a minimal change in meridian curvature, which has been designed to maximum draft efficiency, and to provide structural stability to the membrane. This minimal change in curvature presents a different profile for wind loading to be applied to, and potentially a different circumferential pressure distribution. If the cooling tower in question were to be treated as having a cylindrical cross-section when determining wind loads, the pressure distribution would appear more like that determined by Dryden and Hill [10]. In a paper for the Bureau of Statistics, on wind pressure on circular cylinders and chimneys, Dryden and Hill determined that wind pressure was proportional to angles of surface elements to the wind, as shown by Figure 2.4.

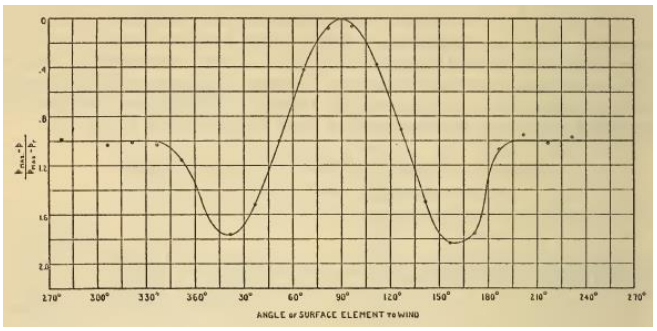

Figure 2.4: Pressure Distribution of Circular Cylinders [10]

The pressure distribution showed that at angles 0° to wind direction pressure coefficients were a maximum, and at angles 90° to wind direction, the pressure coefficients were zero. Taking the sine of the angle to wind, Dryden and Hill showed that the pressure distribution on circular cylinders is closely parabolic, as evident by Figure 2.5.

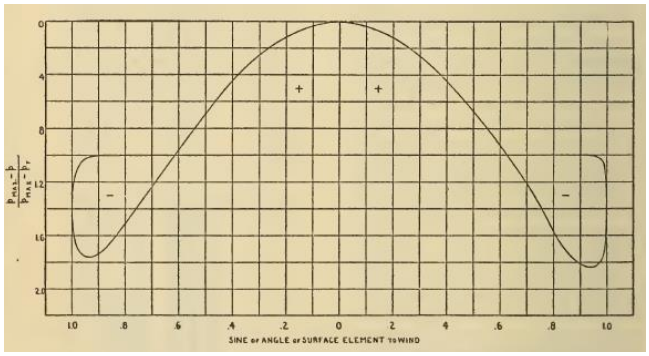

Figure 2.5: Pressure Profile on Circular Cylinders – Sine of Angle to Wind [10]

These observations give an insight into methods of applying wind loads to cooling towers, depending on the assumptions made regarding the cooling towers shape.

2.3 Tensile Membrane Structures

The use of a polymer membrane structure by the QGECE Hybrid Cooling Tower presents an innovative alternative to traditional reinforced concrete structures. The membrane used was a 700 g/m^2, 0.6 mm thick PVC coated polyester [6], which would have been manufactured smaller than the intended final shape, and then stretched into shape by means of prestensioning (or prestressing) the membrane to some percentage of the materials tensile strength. The effect of pretensioning the membrane would induce a uniformly distributed load to the anchoring structure, equivalent to the pretension load. Mollaert and Forster, in the European Design Guide for Tensile Surface Structures [11], suggests that pretension should not be less than 2.5% and not greater than 6% of the tensile strength of the material in both warp and weft directions (longitudinal and transverse weave, respectively) and that PVC coated membranes shall be no less than 1.3%.

Currently, wind loading on tensile membrane structures are based on approximations of applications to flat and spherical shapes. Furthermore, the majority of previous studies have set out to determine wind force coefficients of tensile membrane structures, such as studies by Pun [12] and Takeda et al [13], without making clear distinctions as to the effects of winding loading on such structures. A study conducted by Son [14] was concerned primarily with discerning design analysis aspects of tensile membrane structures. The form factor (ratio of warp to weft stress) of tensioned membranes, along with supporting structure geometry and induced pretension was found to be pertinent to the resulting shape of membranes. Figure 2.6 shows varying membrane forms to these effects, warp to weft ratio varying from 1:1 to 5:1 left to right.

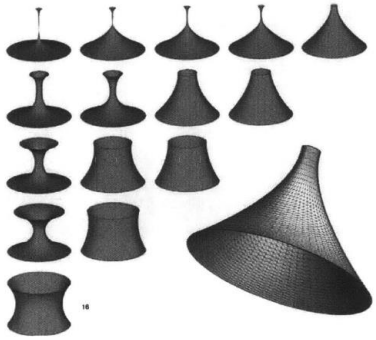

Figure 2.6: Membrane Forms According to Warp:Weft Ratio (1:1 to 5:1, left to right) [14]

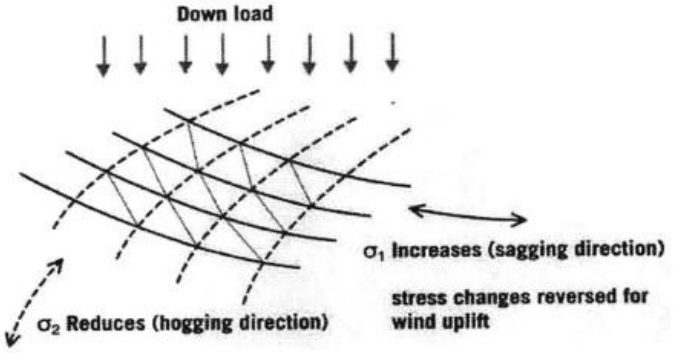

Figure 2.7: Effects of Membrane Loading [14]

When load is applied to tensile membranes non-linear behaviours can be expected to occur, where the curvature of the membrane and loading affects membrane stresses. A membrane under pretension may regain natural equilibrium by changes in membrane geometry and stress, and significant deflections may be expected as a result due to low rigidity and stiffness. Son [14] gave an example applicable to the QGECE Hybrid Cooling Tower, in particular how the weave orientation of membranes under pretension can affect stresses. Analogous to Figure 2.7, the membrane of the QGECE Hybrid Cooling Tower can be envisaged as being pretensioned between top and bottom ring beams, with warp running longitudinally (having an inward curvature) and weft running laterally (having an outward curvature). When a horizontal load is applied externally to the tower, the stress in the warp direction is expected to increase, and the stress in the weft is expected to decrease.

ASCE 55-10, The American Society of Civil Engineers Standard for Tensile Membrane Structures [15] specifies the minimum criteria for the design and performance of tensile membrane structures. An important consideration in the design of tensile membrane structures is the design and specification of membrane connections. Membrane connections can be defined as being fabric-to-fabric, fabric-to-non-fabric, mechanical, or other non-fabric

connections. ASCE 55-10 states that connections are to be designed to transfer all applied and internal forces and moments required by analysis. For use in structures being analysed in this thesis, other non-fabric connections such as cable-to-cable, cable-to-steel, and cable-to-anchorage shall provide for anticipated rotations, shall have enough adjustability to maintain proper tension forces, and shall allow for long term effects, and shall take into consideration eccentricities in the connection details, as stated by ASCE 55-10. Loads to be considered for tensile membrane structures include; dead loads, which shall consist of; the weight of the membrane, and the weight of reinforcement and joining systems, and wind loads, which shall be determined in accordance with applicable standards, such as AS1170.2.

2.4 Review of Relevant Standards

The following section presents standards, which will be relevant within the scope of the thesis, and are to be reviewed to ensure design practices and guidelines are adhered to.

2.4.1 AS1170.2: Structural Design Actions – Wind Actions

The Australian/New Zealand Standard for Structural Design Actions – Wind Actions [16] sets out design procedures for determining wind speeds and resulting wind actions to be used in the structural design of structures subjected to wind actions. The general procedure for determining wind actions (W) on structures, as stated by AS1170.2, are as follows:

- Determine site wind speeds.
- Determine design wind speeds from the site wind speeds.
- Determine design wind pressures and distributed forces.
- Calculate wind actions.

Site wind speeds ($V_{sit,\beta}$) defined for the 8 cardinal directions (β) at the reference height of the structure (z) above the ground, as per AS1170.2, shall be determined by Equation 1.

$$V_{sit,\beta} = V_R M_d (M_{z,cat} M_s M_t) \quad (1)$$

where

V_R = regional gust wind speed (m/s)

M_d = wind direction multipliers for the 8 cardinal directions (β)

$M_{z,cat}$ = terrain/height multiplier

M_s = shielding multiplier

M_t = topographic multiplier

The design wind speeds ($V_{des,\theta}$) orthogonal to the structure are to be taken as the maximum site wind speed linearly interpolated between cardinal points within ±45° to the orthogonal direction being considered, as depicted by Figure A.1 of Appendix A.

The design wind pressure (p), in pascals, as per AS1170.2, shall be determined for structures and parts of structures as given by Equation 2.

$$p = (0.5\,\rho_{air})\left[V_{des,\theta}\right]^2 C_{fig} C_{dyn} \quad (2)$$

where

ρ_{air} = density of air, 1.2 kg/m^3

$V_{des,\theta}$ = building orthogonal design wind speeds (θ = 0°, 90°, 180°, and 270°)

C_{fig} = aerodynamic shape factor

C_{dyn} = dynamic response factor (1.0 except where structure is dynamically wind sensitive)

The aerodynamic shape factor (C_{fig}) is detrimental in the determination of the design wind pressures and distributed forces, and is pertinent to the shape of the structure being analysed. The aerodynamic shape factor, as per AS1170.2, for the specific surfaces when assuming a cooling tower shall be treated as a circular bin, silo, or tank. For the walls of isolated circular bins, silos and tanks of circular-cross section, the aerodynamic shape factor shall, as per AS1170.2, be equal to the external pressure coefficients ($C_{p,b}$) as a function of the angle θ_b (refer to Figure 2.8), given by Equation 3.

$$C_{fig} = C_{p,b}(\theta_b) = k_b C_{p1}(\theta_b) \quad (3)$$

where

the cylinder is standing on the ground or supported by columns of a height not greater than the height of the cylinder (c), as shown by Figure 2.9.

c/b is to be in the range 0.25 to 4.0

θ_b = angle from the wind direction to a point on the wall of the circular bin, silo or tank, in degrees

k_b = factor/function for circular bin, given by Equations 4, and 5

= 1.0 for $C_{p1} \geq -0.15, or$

= $1.0 - 0.55(C_{p1}(\theta_b) + 0.15)\log_{10}(c/b)$ for $C_{p1} < -0.15$ (4)

$$C_{p1}(\theta_b) = -0.5 + 0.4\cos\theta_b + 0.8\cos 2\theta_b + 0.3\cos 3\theta_b - 0.1\cos 4\theta_b - 0.05\cos 5\theta_b \quad (5)$$

For calculating the overall drag force on the wall section of circular bins, silos and tanks, AS1170.2 specifies that C_{fig} shall be taken as 0.63. This arises from an integration of the along-wind component of the normal pressures given by Equations 4 and 5, and by the area under the curve given by the graphical representation (Figure 2.10) of external pressure coefficients for circular bins, silos and tanks of unit aspect ratio. A plot of the QGECE Hybrid Cooling Tower pressure distribution, having an aspect ratio of 1.25, is shown in Figure 2.11.

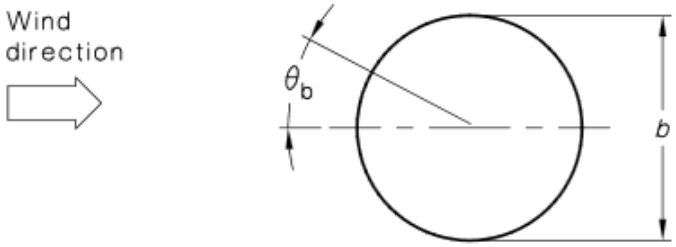

Figure 2.8: AS1170.2 Definition of Angle from Wind Direction

Figure 2.9: AS1170.2 Cylinder Height Definitions

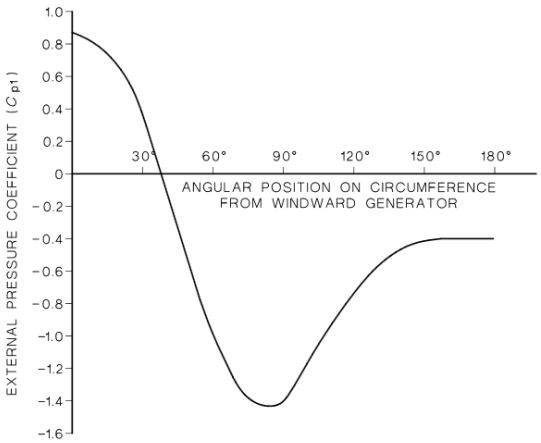

Figure 2.10: AS1170.2 Plot of Pressure Coefficients

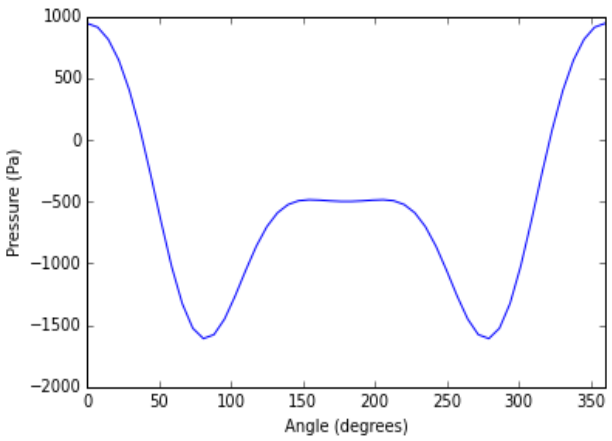

Figure 2.11: QGECE Hybrid Cooling Tower Pressure Distribution

2.4.2 AS4100: Steel Structures

The Australian Standard for Steel Structures [17] sets out the minimum requirements for the design, fabrication, erection, and modification of steelwork in structures in accordance with the limit states design method.

2.4.2.1 Materials

It is specified that yield and tensile strength of steel used in design should not exceed that given in Table 2.1. Additionally, all structural steel, before fabrication, shall comply with the requirements of additional steel standards, as appropriate. For example, AS1163: Cold-formed Structural Steel Hollow Sections will need to be complied with, as the use of hollow sections will fall within the scope of this thesis.

Table 2.1: Strengths of Steels

Grade	Minimum Yield Strength (MPa)	Minimum Tensile Strength (MPa)
C250	250	320
C350	350	430
C450	450	500

Identifying the mechanical properties for cold-formed hollow sections is necessary when defining engineering data and material for FEA structural analysis, as the mechanical properties can affect results such as bending and/or buckling stresses. The QGECE Hybrid Cooling Tower is constructed from grade C350 structural steel.

2.4.2.2 General Design Requirements

The general design requirements state that the aim of structural design is to provide a structure which is stable, has adequate strength, is serviceable and durable, and which satisfies other objectives such as economy and ease of construction. For the scope of the thesis, only the following design aspects and structural analysis methods of AS4100, shall considered and reviewed: loads, member buckling analysis, and connections. Aspects such as elastic analysis plastic analysis, in-depth design for member bending, axial tension and compression, brittle fracture and fatigue were omitted from analysis and investigation.

2.4.2.3 Loads

The design of a structure for the stability, strength and serviceability limit states shall account for the action effects directly arising from loads such as dead, live, wind, snow, ice and earthquake, with loads effecting cooling towers in Australia being mostly dead and wind loading, and are specified in AS1170.1 and AS1170.2 respectively. Additional loads that may

affect the stability, strength or serviceability of the structure that may be taken into account for cooling towers in Australia are dynamic loading effects, and construction loading.

2.4.2.4 Member Buckling Analysis

Equation 6 shall determine the elastic buckling of a member for particular end constraints provided by the surrounding frame.

$$N_{om} = \frac{\pi^2 EI}{(k_e l)^2} \quad (6)$$

where

N_{om} = elastic buckling load of a member

E = Young's modulus

I = cross-sectional moment of area of a member

k_e = member effective length factor

l = member length

Values of member effective length factor for various end constraints are shown in Figure 2.12

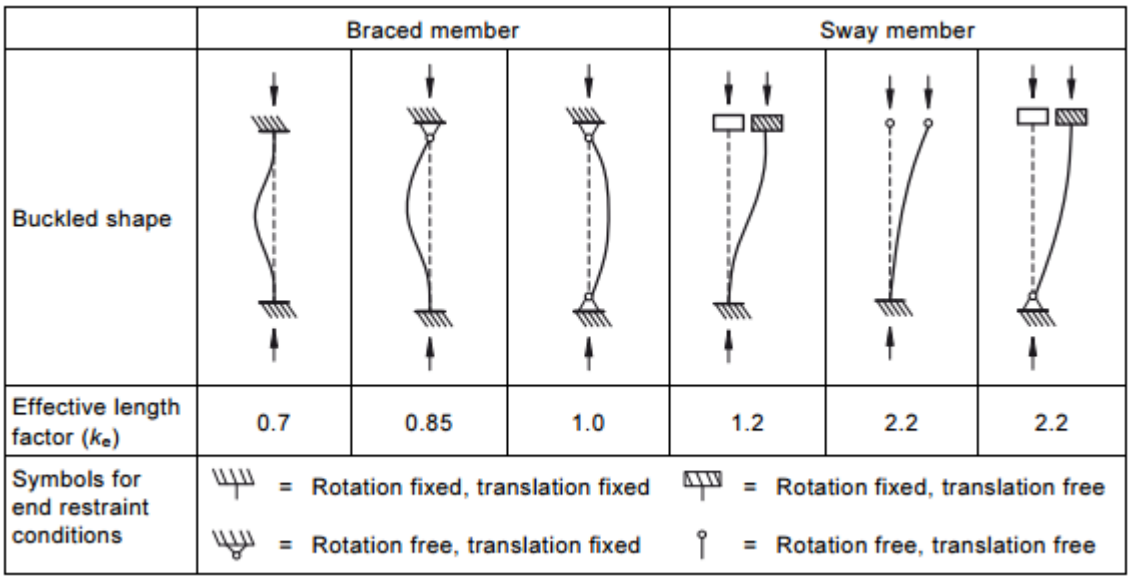

Figure 2.12: Effective Length Factor for Member End Constraints

2.4.2.5 Connections

Connection elements are said to consist of connection components, such as; cleats, gusset plates, brackets, connecting plates, and connectors, such as; bolts, pins, welds. Connections need to be proportioned appropriately, and capable of transmitting calculated design action effects. Three types of construction classify connections; rigid, semi-rigid, and simple. A rigid connection is defined as there having no significant influence on the distribution of action

effects. A semi-rigid connection is defined as providing a predictable degree of interaction between members. A simple connection is defined as being capable of deforming to provide the required rotation at the element.

Each element in a connection needs to be designed so that the structure is capable of resisting all design actions. Connections carrying design action effects shall be designed to transmit the greater of; the design action in the member, or the minimum design action effects expressed as the value of the factor times the member design capacity required by the strength limit state, as specified by Clause 9.1.4 of AS4100.

Connection components such as cleats, gusset plates, brackets, and connecting plates, shall be designed as per AS4100 as follows:

- Clause 5.11.3 for connection components subject to shear.
- Clause 7.2 for connection components subject to tension.
- Clauses 6.2.1 and 6.3.3 for connection components subject to compression.
- Clauses 5.2.1 for connection components subject to bending.

Connectors such as bolts, pin connections, and welds, shall be designed and assessed as per AS4100 as follows:

- Clauses 9.3 and 9.4, for the design of bolts and assessment of the strength of a bolt group, respectively.
- Clause 9.5 for the design of a pin connection.
- Clause 9.6 for the design details for bolts and pins.
- Clauses 9.7 and 9.8, for the design of welds and assessment of the strength of a weld group, respectively.

2.4.3 AS1163: Cold-formed Structural Steel Hollow Sections

The Australian/New Zealand Standard for Cold-formed Structural Steel Hollow Sections [18] specifies the requirements for the production and supply of cold-formed, electric resistance-welded, steel hollow sections used for structural purposes. It considers three strength grades, as defined in AS4100, with or without impact properties that are suitable for welding, and are the same as those shown in Table 2.1. Appendix D of AS1163 provides a list of common cold-formed structural steel hollow sections available in Australia and New Zealand, and provides section designations, dimensions, and cross-section and mass properties. The list provides properties for the three most common type of structural steel hollow sections, and the only sections presented in AS1163, which are; circular hollow sections (CHS), rectangular hollow

sections (RHS), and square hollow sections (SHS). The scope of this thesis shall only pertain to the designation and use of circular hollow sections for structural members.

Circular hollow sections are designated by; the nominal outside diameter d_o, and the nominal thickness t, commonly expressed as $d_o \times t$ CHS in millimetres in manufacturer product catalogues. Figure 2.13 shows the designation of circular hollow sections.

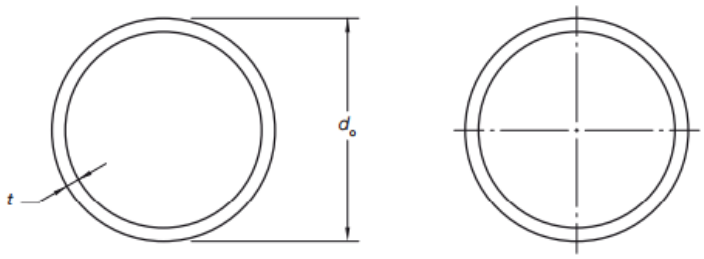

Figure 2.13: Circular Hollow Section

The QGECE Hybrid Cooling Tower utilises two circular hollow sections; designation 323.9 × 9.5 CHS for the ring beams, and designation 273.1 × 6.4 CHS for the vertical support columns.

2.4.4 AS3569 & AS2759: Steel Wire Ropes

AS3569, the Australian Standard for Steel Wire ropes – Product Specification [19] specifies the minimum requirements for the manufacture and testing of stranded ropes for general purposes, including lifting equipment such as cranes and hoists. It also presents minimum breaking forces and dimension for common sizes, grades and types of constructions of stranded rope for slings.

Four tensile grades of wire are specified, shown in Table 2.2, which are defined to enable the minimum breaking force of the wire to be achieved.

Table 2.2: Wire Rope Tensile Grades

Wire Grade	Tensile Strength Grade Range (N/mm^2, MPa)
1570	1370 to 1770
1770	1570 to 1960
1960	1770 to 2160
2160	1960 to 2160

The minimum breaking force (F_{min}) of a specified steel wire rope is a specified value, below which the measured breaking force (F_m) is not allowed to fall in a prescribed breaking force test. If the need for steel wire ropes is necessary in a cooling tower design, a selection can be

made, according to required breaking force, from the tables of minimum breaking forces for various rope classes, sizes and grades, specified in Appendix C of AS3569.

AS2759, the Australian Standard for Steel wire rope – Use, operation and maintenance [20] specifies the recommended procedures for the selection, storage, handling, maintenance, use, inspection, and discard of steel wire ropes. For cooling tower structures being investigated in this thesis where steel wire rope may be used (in alternative structural geometries and construction methods) factors such as the intended use, longevity and maintenance/inspection need to be considered. AS2759 states that the selection of the most suitable steel wire rope for a particular purpose is governed largely by practical experience and generally calls for the best compromise in rope qualities to cope with loading, the type of equipment and the working conditions. When long rope life is required, a high design factor and high bending ration should be adopted.

Depending on the selection of steel wire rope, a combination of particular properties can be obtained. The following is given in AS2759 to assist in the correct choice of rope:

- Where abrasive conditions are encountered, rope constructions with the largest possible outer wires or rope surface compatible with the required flexibility should be used.
- Where the rope can be anchored at both ends to prevent rotation, the use of Lang's lay ropes is recommended for conditions of heavy wear and severe flexing.
- Where rope is subject to heavy loading and flexing over small sheaves or drums, a rope with a wire rope core should be used.
- Where ready and regular maintenance is difficult, galvanized wire ropes should be used.
- An increased number of outer strands with smooth surfaces minimizes wear on sheaves, drums and rope.

Steel wire rope should be regarded as a wearing component, as it is not possible for any rope to have an infinite life without necessary maintenance, or replacement at some point during service. Consequently, maximizing service life of a wire rope is dependent on regular conditional inspection. Inspection should be carried out by competent persons and in accordance with measures stated in AS2759. The frequency of inspection will be influenced by the nature of the equipment and the intended use and working conditions.

Alternative construction methods investigated in later sections (Section 2.6) and the presentation of alternative structural geometries (Section 5.4) specify the use of steel wire rope in conditions where wire rope shall be either running or standing. As such, wire rope needs to be selected for the working conditions and loads appropriate for the application, and special

consideration needs to be made on the maintenance/inspection required of the intended application.

2.4.5 AS3600: Concrete Structures

The Australian Standard for Concrete Structures [21] specifies design procedures for concrete building structures and members that contain reinforcing steel, as well as the minimum requirements for plain concrete pedestals and footings.

Within the context of the thesis, and the cooling towers being investigated and analysed, concrete footings need to be designed to carry required design loads. For this to be achieved, the way that the footing, of a structural element or component, supports the reaction of a load needs to be considered. For example, if there is a sufficient moment produced in the structure because of wind loading, the ground supports could effectively act to pull up on the foundations, and design would need to be carried out to accommodate such reaction. Similarly, investigation into alternative construction methods and structural geometries introduce elements where additional concrete footings will be necessary, and there may be other load reactions that need to be considered for the design of concrete footings. In these cases, particularly for foundations of a winch anchor (see Section 2.6), foundations may need to be designed to account for some combination of upward and lateral loading.

AS3600 specifies that plain concrete pad footings supported by the ground shall have a minimum depth of 200 mm, and that when calculating the strength of the footing, the entire cross-section needs to be considered, assuming the depth is 50 mm less that of the minimum depth.

For footings where loads may experience an "upward pulling" tensile load, it may be appropriate to consider the design bending strength of concrete footings. The design bending strength of concrete footings is stated by AS3600 to be based on a linear stress-strain relationship in both tension and compression, and should be taken as ϕM_{uo}, where ϕ is the capacity reduction factor given in Table 2.2.2 of AS3600, and M_{uo} is the ultimate bending strength at critical sections. M_{uo} is calculated using Equation 7, using the characteristic flexural tensile strength $f'_{ct.f}$ of concrete at 28 days which is given by Equation 8. The critical section can be taken as halfway between the face of the column and the edge of the base plate for a steel column and base plate.

$$M_{uo} = 1.2\left[Z\left(f'_{ct.f} + P_e/A_g\right) + P_e e\right] \quad (7)$$

where

Z = section modulus of the uncracked cross-section, referred to the extreme fibre at which flexural cracking occurs

P_e = total effective prestress force allowing for all losses of prestress

e = eccentricity of the prestressing force, measure from the centroidal axis of the uncracked section

$$f'_{ct.f} = 0.6\sqrt{f'_c} \quad (8)$$

where

f'_c = the characteristic compressive strength of concrete at 28 days of the specified strength grade of concrete (common grades and properties given in Table 3.1.2 of AS3600

For footings where loads may experience some sort of lateral laod, it may be appropriate to consider the design shear stress of concrete footings. The design shear strength of concrete footings is determined using either Equation 9, Equation 10 or both. The design shear strength shall be taken as ϕV_u, where Equation 10 is calculated when a member acts as a one-way member, and a shear failure can occur across the width of the rectangular cross section (b) of the member.

$$V_u = 0.15bD(f'_c)^{1/3} \quad (9)$$

where

D = overall depth of cross-section in the plane of bending, or

= depth or breadth of the symmetrical prism as appropriate

The critical section for one-way shear is specified to take $0.5D$ from the face of the support.

Equation 10 calculates the design shear strength when a shear failure can occur locally around a support or loaded area.

$$\phi V_u/[1 + (uM^*/8V^*aD)] \quad (10)$$

where

$$V_u = 0.1uD(1 + 2/\beta_h)\sqrt{f_c'} \leq 0.2uD\sqrt{f_c'} \quad (11)$$

M^* = design bending moment at a cross-section

V^* = design shear force at a cross-section

u = effective length of the shear perimeter (see Figure 9.2.1(A) of AS3600)

a = dimension of the critical shear perimeter, which is parallel to the direction of bending being considered (see Figure 9.2.1(B) of AS3600)

β_h = ratio given in Clause 9.2.1.5 of AS3600

2.5 Crane Selection

The construction and erection of large-scale structures will nearly always depend on the use of cranes, the selection of which is important for optimising factors such as productivity, safety, and cost. The American Institute of Steel Construction (AISC) [22] presents a teaching aid for use in construction classes to teach the principles that govern crane selection. The AISC classify at least five types of cranes, defined and listed as follows:

- Rough terrain; designed for unimproved worksites, roadable for short distances, four steering modes, pick and carry capability, three position outriggers.
- Truck mounted; can be driven at highway speeds, limited off-road capability, capable of multiple lift tasks in one day, hydraulic booms allow for fast setup but weight reduces lifting capability.
- All terrain; combines features of rough terrain and truck mounted cranes, off-road capable, all-wheel steering, highway speeds.
- Crawler lattice; high-capacity long reach lifts, pick and carry capability multiple attachments provide flexibility in boom configuration.
- Tower; used when space is at a premium, up and over reach, moving counterweight balanes load, fixed foundation or crawler with attachment.

The AISC specifies critical criteria for selecting cranes that includes factors such as; the available space for a crane to operate on a jobsite, the working range of a cranes ability to reach, load capacity charts for all boom configurations at all ranges, crane availability, and the number of lifts required for a job. This criteria indicates the significant importance of crane selection, and how selecting the correct crane can; improve production efficiency, ensure a safe work environment is created, and optimise costs incurred during the construction process of a project.

Han et al. [23] developed a framework for the selection of cranes for large scale industrial construction projects which aimed at developing a decision support system to enhance the crane selection process.

Table 2.3: Categories and Factors Affecting Crane Selection

Category	Factors
Equipment and cost	Cost (sub-factors: rental, transportation, installation expenses, etc.)
	Installation & Disassembly (sub-factors: time/difficulties in installation, etc.)
	Maintenance & Depreciations (sub-factors: average breakdown cycle, etc.)
	Additional Safety Features/Technology (sub-factors: operators skill, etc.)
Location and site	Weather (sub-factors: daily wind conditions, etc.)
	Availability (sub-factors: crane availability, etc.)
	Space (sub-factors: space requirements for installation, etc.)
	Support System (sub-factors: depreciation of support system, etc.)
	Transportation (sub-factors: transportation of crane, etc.)
Environmental impact	Energy (sub-factors: type of crane power, etc.)
	Health (sub-factors: noise & dust, etc.)
	CO_2 Emission (sub-factors: CO_2 emission at operation, etc.)
	Neighbour impact (sub-factors: privacy, etc.)

The framework highlights categories, factors, and sub-factors, an example for which is shown in Table 2.3, which were used in a decision support matrix used to select an optimal crane. Categories and factors are ranked based on a questionnaire feedback system, and also by the importance of each category or factor. Sub-factors are then ranked by the suitability for the type of crane for a given sub-factor.

A crane selection matrix mechanism was developed to calculate the sub-factor values for each type of crane, which was then used to calculate total scores for each crane type to select the most suitable crane. While detailed, the framework developed by Hans et al. relies on an opinion based ranking system for ranking each sub-factor, with far too many variables. The questionnaire based approach to ranking categories and factors may be more effective in giving persons using the framework an unbiased approach to determining the most suitable crane for the construction project. Additionally, the tools presented by the AISC in comparison to that developed by Hans et al., are seemingly more simplified and may be a more suitable approach to take when selecting the most appropriate crane by making a selection on specific criteria.

2.6 Construction Methods

The use of cranes in the erection of structures can amount to large construction costs, particularly if the size of the structure sets a specific requirement on the number of cranes needed, the types of cranes needed, and if specialist cranes are required for one off lifts. Armato [24] outlines common scenarios as to why cranes might be suitable, and presents several alternatives to cranes. Some common scenarios where cranes may be impractical include:

- The plane layout; where it is important to consider the plane of each crane to avoid unnecessary time wasted if one crane was waiting for another to get out of the way.
- Size; where the use of a particular crane might not be appropriate for the project, or if all work is done on or near ground level, a crane could present an inefficient use of time.
- Local climate; heavy winds may affect lifting loads and the stability of the crane, and ground pressure and stiffness may limit the maximum weight of a crane.

Some alternatives to cranes include:

- Modular lift towers; which comprise of a modular column and lacing framework used in a tower system, and can be setup in the same time as cranes, with mobilisation costs low relative to lifting capacity.
- Excavators/Telehandlers; where excavating attachments may be replaced in favour of lifting attachments.

Another construction method to using cranes, particularly for erecting towers, is via a tilt-up tower method, which is a method commonly used to erect domestic and small-scale wind turbines, measurement towers, and amateur radio masts. The method uses similar principles to that of dragline booms and luffing towers. Tilt-up towers are designed so that they can be lowered by tilting the tower with a gin pole and winch, as describe by Stapleton et al. [25], and shown in Figure 2.14.

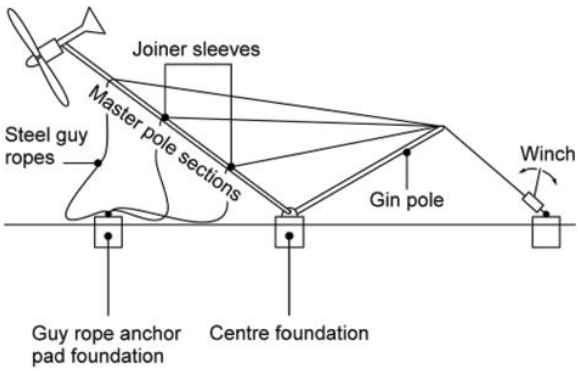

Figure 2.14: Example of a Tilt-Up Tower

In a publication focusing on reducing household energy consumption in Australia, Stapleton et al. presented methods for installing domestic wind turbines. Three main types of tower were compared, including the tilt-up, as well as guyed lattice and freestanding towers, which could either be lattice or monopole. One of the factors that was compared between the tower types was the cost associated with installing each. It was shown that freestanding towers installed using cranes are the most expensive, guyed lattice installed using cranes the least expensive crane, and tilt-up towers have mid-range costs. The comparison presented only considers monopole towers; the cooling towers being investigated in this thesis are considerably more complex, which may require multiple cranes for lifts, and specific cranes for one-off lifts. Therefore, the difference in cost between using a tilt-up tower, to other tower and lift methods may be more comparable for applications presented by this thesis. An important factor to take into consideration when selecting a tower type or erection method is the required base, and the area of the building footprint. Freestanding towers require the least cleared area, needing a concrete foundation that is 7-10% of the tower height. Fixed guyed towers require a minimum cleared area equivalent to a guy radius of 50-80% of the tower height. Tilt-up towers require a smaller guying radius, 35-60% of the tower height, however the minimum cleared area needs to accommodate the height of the tower when it is lying down prior to being tilted. The gin-pole of a tilt-up tower is also suggested to be 75-100% of the guy wire radius.

3 METHODOLOGY

The following chapter shall set forth the methodology used for defining and calculating loads and load cases for cooling towers within the scope of the thesis. The determination and application of structure pretension loads are presented, as are the determination and application of structure wind loading. Validation of existing analysis has been conducted, and a benchmark of design has been produced as a result. Methods of analysis of alternative construction methods are also presented. The following assumptions were made throughout the presented methodology:

- Cooling tower shape shall be treated as cylindrical when calculating drag forces.
- Wind loads were applied using a parabolic load, based on findings from Dryden and Hill [10].
- Wind loading only affected the windward half of the cooling tower.
- Maximum pretension loads were taken as 5% of the membranes specified tensile strength, as specified by the Euro Design Guide for Tensile Surface Structures [11].

3.1 Pretension Loads

The pretension load transmitted to the tower structure due to stretching the membrane into shape during construction was determined by examining the material properties of the membrane. The membrane was manufactured from a Mehler FR 700 Type I 7205 PVC [6]. Important material properties are shown in Table 3.1.

Table 3.1: PVC Membrane Material Properties

Material Property	Mehler FR 700 Type I 7205
Total Weight (g/m^2)	700
Fabric Thickness (mm)	0.6
Tensile Strength (warp/weft) (N/50mm)	3000/3000

A pretension load (F_t) of 150 N/50 mm or 3 kN/m, was applied to the membrane anchoring structure as a uniformly distributed load as depicted by F_t in Figure 3.1, under assumptions made at the beginning of this chapter.

3.2 Wind Loads

Structural wind loads were determined using AS1170.2 standards. The maximum design wind speed and design wind pressure were determined to be 43 m/s and 700 Pa, using Equations 1

and 2 of Section 2.4.1, respectively. Significant factors and multipliers used in the determination of the site wind speed and design wind pressure are shown in Table 3.2.

The site wind speed was given by Equation 1 from Section 2.4.1;

$$V_{sit,\beta} = V_R M_d (M_{Z,cat} M_s M_t)$$

where

V_R = regional gust wind speed (m/s)
M_d = wind direction multipliers for the 8 cardinal directions (β)
$M_{z,cat}$ = terrain/height multiplier
M_s = shielding multiplier
M_t = topographic multiplier

and the design wind pressure was given by Equation 2 from Section 2.4.1.

$$p = (0.5\rho_{air})\left[V_{des,\theta}\right]^2 C_{fig} C_{dyn}$$

where

ρ_{air} = density of air, 1.2 kg/m^3
$V_{des,\theta}$ = building orthogonal design wind speeds (θ = 0°, 90°, 180°, and 270°)
C_{fig} = aerodynamic shape factor
C_{dyn} = dynamic response factor (1.0 except where structure is dynamically wind sensitive)

Table 3.2: Significant Factors/Multipliers in Determining Design Wind Speed and Pressure

Factor/Multiplier	Assumed Value and Justification
V_R	38m/s as per Section 3.2 of AS1170.2
M_d	0.95 as per Section 3.3 of AS1170.2
$M_{z,cat}$	1.19 to 0.75 for Terrain Categories 1 to 4 as per Section 4.2 of AS1170.2
M_s	1.0 shielding not applicable as per Section 4.3 of AS1170.2
M_t	1.0 for $H/2L_u < 0.05$, where H is the height of, and L_u is the horizontal distance upwind to, crest/hill/escarpment as per Section 4.4 of AS1170.2
C_{fig}	0.63 as per Appendix C5 of AS1170.2
C_{dyn}	1.0 as per Section 2.4 of AS1170.2

3.3 Application of Wind Loads

The wind load acting on the cooling tower, 700 Pa, was resolved into a drag force acting on the tower membrane by multiplying the cross-sectional area of the tower membrane, with dimensions 15 m high x 12 m wide. This equated to a drag force of 126 kN acting on the membrane. This drag force was resolved into horizontal and vertical loads transmitted to the membrane anchorages.

To determine the forces transmitted through the membrane anchorages to any connecting tower structure, the drag force was halved to represent the horizontal forces acting on the two opposing membrane anchor points. The horizontal force was then resolved into a vertical force acting equal and opposite to the membrane anchor points, determined from the tangent line acting through the end of the hyperboloid of the tower membrane, as shown in Figure 3.1.

The horizontal ($F_{d/2}$) and vertical ($F_V = \frac{F_{d/2}}{\tan\theta}$) forces transmitted through the membrane anchorages to any connecting tower structure were determined to be 63 kN and 96 kN, respectively. These forces would act only on the windward facing side of the cooling tower and were applied as such when analysed using FE software. The wind loads were applied at different structure orthogonal angles, to represent wind acting from different directions, depending on tower geometry as depicted by Figure 3.2.

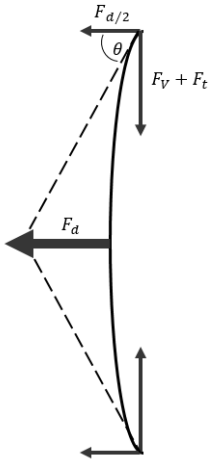

Figure 3.1: Representation of Wind Load Forces

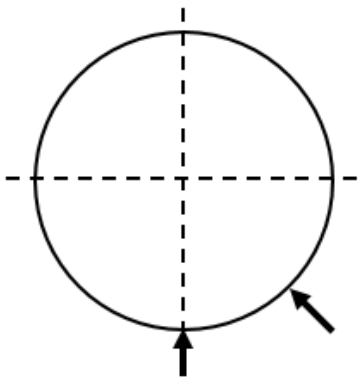

Figure 3.2: Wind Load Directions Indicative of a Symmetric Structure

The wind loads were applied using a parabolic load profile, based on findings from Dryden and Hill [10], who suggest that the wind pressure distribution along circular cylinders is roughly parabolic. The parabolic wind load profile was applied to the circumferential length of the windward half of the tower. Hence, the horizontal wind load $F_{d/2}$, equated to a circumferential wind load of 3.342 kN/m for a circumferential length of 18.85 m. The premise of the parabolic

load profile is for the circumferential wind load to be distributed such that the windward most part of the tower will exhibit the largest fraction of the load. The sides of the tower will exhibit a smaller fraction of the load, while the net total circumferential wind load will remain the same, as depicted by Figure 3.3.

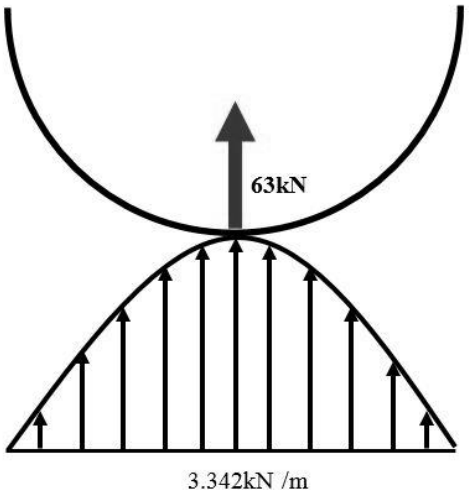

Figure 3.3: Parabolic Load Profile

The fraction of circumferential wind load distribution was determined graphically, by applying a mean circumferential load. The mean circumferential load was used to express how the net total circumferential wind load would be applied if a simple uniformly distributed load profile was used as opposed to a parabolic load profile, as shown in Figure 3.4. It was determined that the circumferential wind load would be distributed so that the front of the tower (tip of the parabolic load profile) will experience double the net circumferential wind load, while the sides of the tower (edges of the parabolic load profile) will experience close to none of the net circumferential wind load.

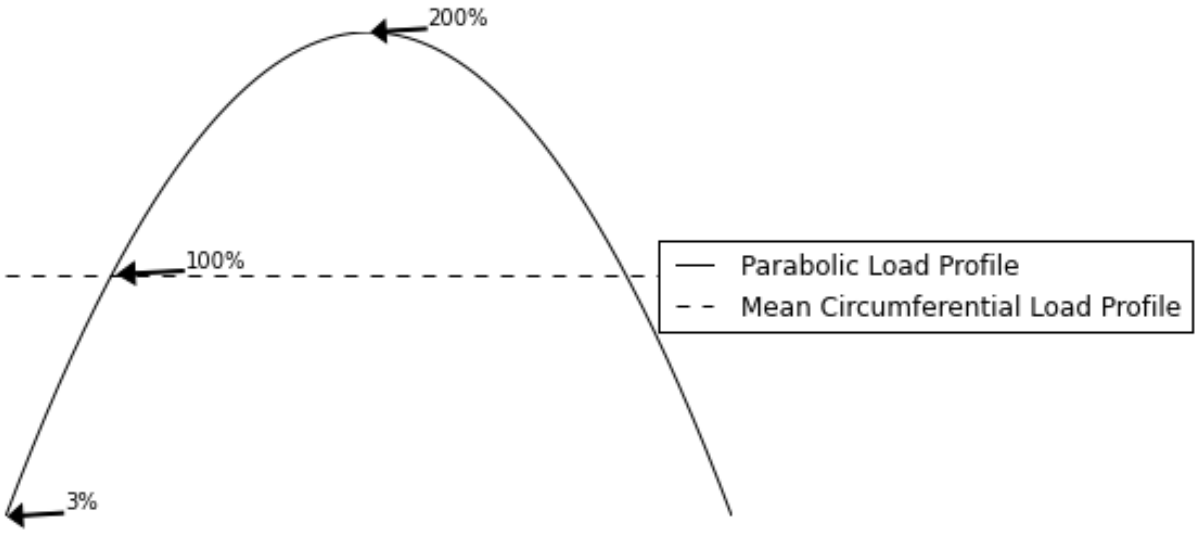

Figure 3.4: Parabolic Wind Load Distribution

The parabolic load profile was applied in ANSYS Workbench, by dividing the load profile into sections, and applying a line pressure, which is defined in the ANSYS Mechanical User Guide [26], as a load applied as a distributed force on one edge only, using force density loading in units of force per length. The load profile section would apply a percentage of the net total circumferential load, according to the fraction of the load distribution for that particular section. The percentage distribution across the entire load profile can be referred to in Appendix B.

3.4 Validation Analysis

A comparative study to validate the structural FEA results of Shaharuddin's previous analysis on the QGECE Hybrid Cooling Tower was conducted. In an attempt to validate the previous analysis, an FE model was recreated to endeavour to replicate and ascertain what assumptions were made in the previous analysis, and to determine what boundary conditions were used, and how they were implemented. Results for the validation analysis are shown in Section 5.1. The approach taken in conducting the comparative validation study was as follows:

- Geometry was constructed as per the previous analysis, which took dimensions from engineering drawings of the QGECE Hybrid Cooling Tower.
- Boundary conditions were applied to replicate those defined by the previous analysis.
- Analysis settings were applied as per the previous analysis.
- Simulations were conducted, and results were analysed.
- Geometry and boundary conditions were adjusted until simulation results converged to that of the previous analysis.

Once simulation results have converged to that of the previous analysis, observations can be made to determine if there are any disparities in the models for the previous analysis and validation analysis.

3.5 Benchmark Analysis

By accounting for the oversights concluded from the comparative study, and by conducting additional FE analysis in accordance to relevant standards and procedures outlined in this section, a benchmark analysis was conducted to develop a benchmark of design, and several limiting factors, which would be used to compare against alternative designs developed throughout the thesis. Imperative in conducting the benchmark analysis was validating the FE simulation results. This was achieved by analysing the sum of horizontal reaction forces at the cooling tower ground supports, where the total horizontal reaction force should be approximately equal to the total wind drag force of 126 kN.

3.6 Analysis of Alternatives

3.6.1 Tilt-Up Tower Feasibility

During investigation of alternative construction methods, the tilt-up tower method was considered the most promising for use as an alternative construction method for cooling towers within the scope of this thesis. To determine if a tilt-up tower would be appropriate, a feasibility analysis was conducted to determine if the method would be possible without the aid of a gin pole. The analysis was conducted primarily using FE simulations in ANSYS Workbench, with the support of rudimentary analytical calculations, and simplified truss analysis to aid in validating FE analysis.

Analytically, the tilt-up tower was examined using a basic two dimensional truss analysis of a simplified structural geometry. The truss analysis examined the nodal forces that were indicative of the axial force in each structural member throughout the erection procedure, the erection procedure being all stages from the tower being at an initial position (on the ground) to a final position (fully erect). Table 3.3 defines the key terms and variables used in conducting the truss analysis, and is complemented by Figure 3.5. The winch cable used in the tilt-up tower method was also designed and analysed, using methods defined later, in Section 3.6.2.

Table 3.3: Key Terms and Variables Used in Truss Analysis of Tilt-Up Tower

Term/Variable	Definition
h_{tower}	The height of the tower when fully erect
$h_{erected}$	The height of the tower at that stage of the erection procedure
$\theta_{erected}$	The angle between the ground and tower columns at the erection height
$\theta_{winch}, \alpha, \beta$	The angle between the ground and the winch member (cable) during erection
n_{offset}	The horizontal distance between member nodes at the erection height and the tower height
x_{winch}	The horizontal distance between the winch node and the tower connection node at the tower height
$x_{winch,max}$	The horizontal distance between the winch node and the tower connection node at the erection height
d	The tower diameter

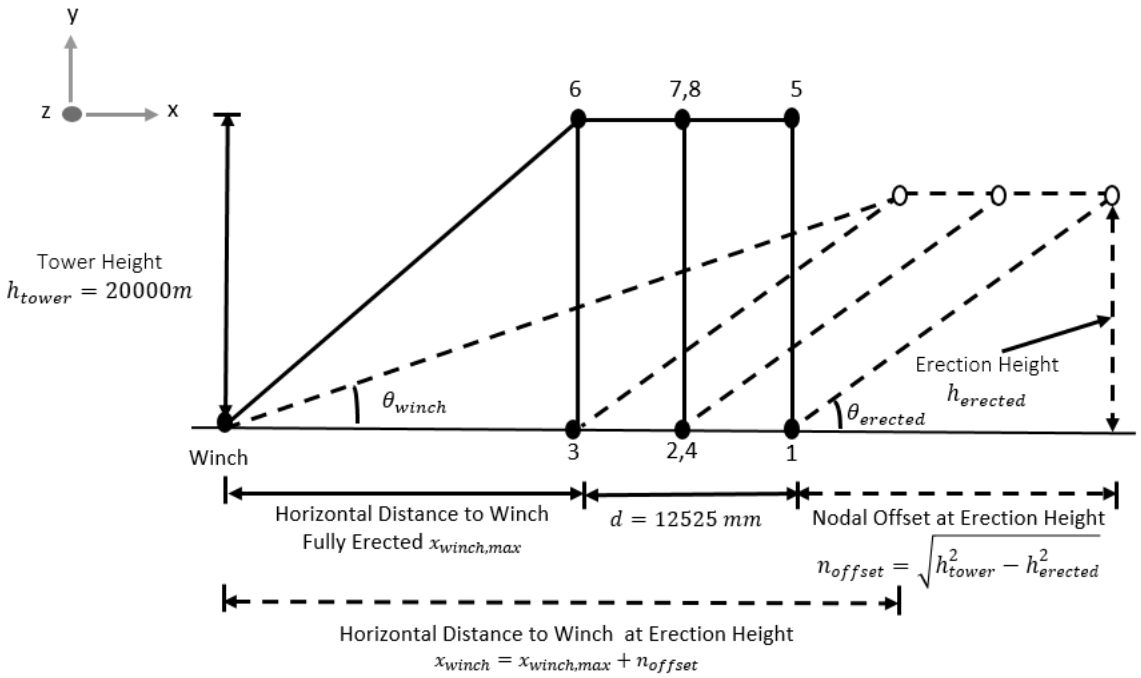

Figure 3.5: Schematic of Key Terms and Variables Used in Analysis of Tilt-Up Tower

The terms and variables were then used to develop a series of equations, which identified and calculated the nodal reaction forces, indicative of the axial force in each structural member. Figure 3.6 shows how the nodal forces in each member were defined. The equations for each nodal force were developed as a function of the erection angle, so that the nodal forces could be calculated for the entire erection procedure, for erection angles of 0° to 90°. Refer to Appendix C for the set of equations defining each nodal force.

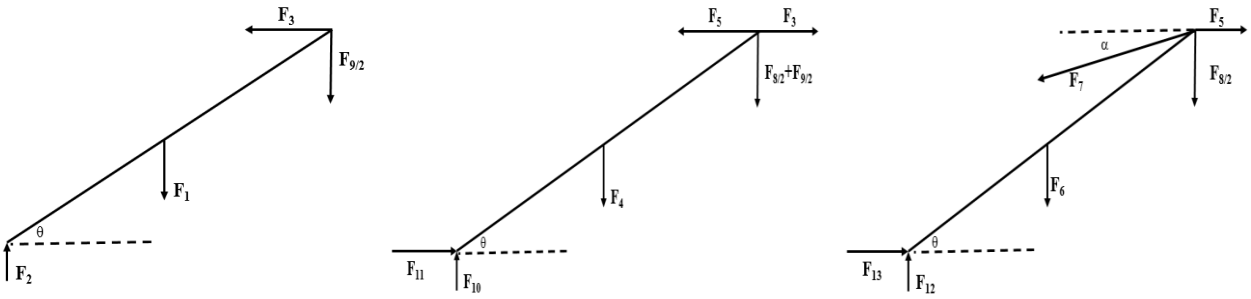

Figure 3.6: Schematic of Tilt-Up Tower Nodal Forces

Results from the initial analysis of the tilt-up tower without a gin pole led to the need for an additional analysis to be conducted to determine if the method would be feasible with the aid of a gin pole. Analytically, the same approach was taken as that of the analysis without the gin pole, however a few additional terms, variables, and equations for the nodal reaction forces were developed. The additional terms and variables are shown in Table 3.4, and are complemented by Figure 3.7. The extra set of equations defining the nodal forces associated with the gin pole are shown in Appendix C.

Table 3.4: Key Terms and Variables Used in Gin Pole Analysis

Term/Variable	Definition
L_{gin}	The length of the gin pole
H_{gin}	The height of the gin pole at the erection height
θ_{gin}	The angle between the gin pole and tower columns (fixed)
β_{gin}	The angle between horizontal and the winch cable, for the winch cable span between the gin pole and tower column

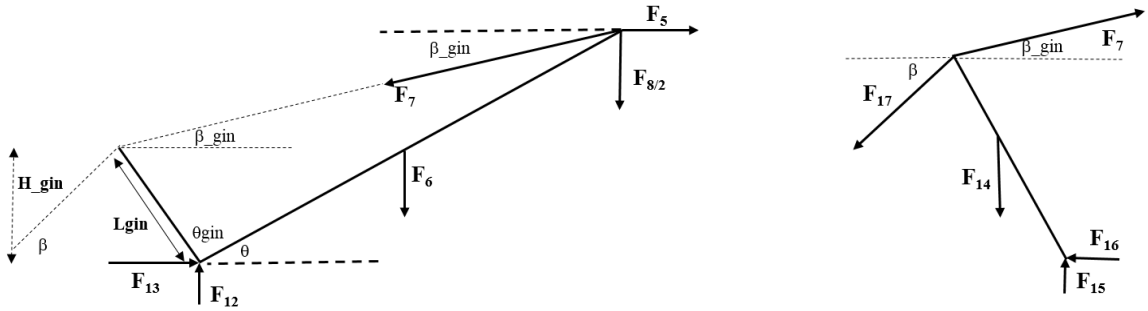

Figure 3.7: Schematic of Gin Pole Nodal Forces

The addition of a gin pole would require a specific design analysis and criteria. A design buckling load would need to be defined as a failure criteria for the gin pole. The gin pole can be considered to have fixed-pinned braced column end constraints, as the base of the gin pole is fixed to the tower, and the top may be assumed to rotate under the winch cable which would act as a brace as the tower is erected. The design buckling load was determined to be 580 kN for a 15 m pole. Design calculations are shown in Appendix D.

3.6.2 Alternative Structural Geometries

Figure 3.8 introduces the two alternative cooling tower structural geometries that are to be investigated and analysed.

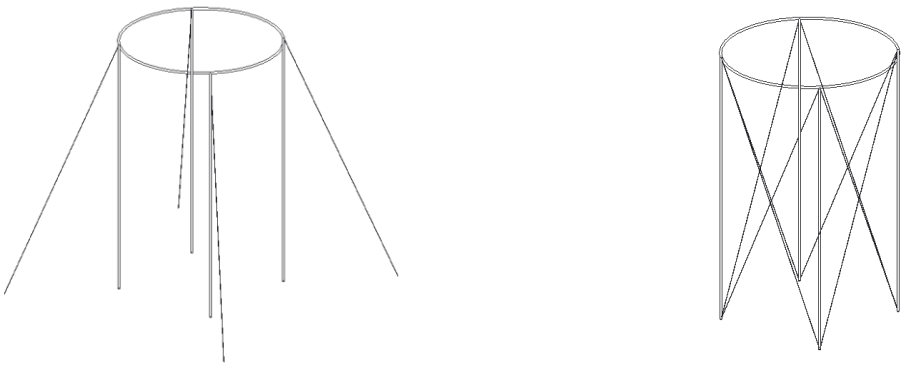

Alternative A (Externally Guyed) **Alternative B (Internally Guyed)**

Figure 3.8: Alternative Structural Geometries

To accommodate the tilt-up method, alternative tower geometries were investigated and analysed. Analysis was conducted exclusively using static structural FE simulations in ANSYS Workbench. The analysis applied static structural wind and pretension loads, in accordance with relevant standards, where loads were applied as specified in Section 3.1 and Section 3.3.

Changes proposed to the original structure in order to accommodate the tilt-up method, necessitated redefining some design criteria. The pivoting action required of the tower to facilitate the use of the tilt-up method, meant that the design buckling load for column members would need to be re-evaluated to account for new member end constraints. The original structure used braced fully fixed column end constraints, representative of bolted connections, however the alternative structures will need to employ braced pin-pin end constraints (members will be braced by steel wire rope). Wind loads would need to be applied at multiple structure orthogonal angles to account for the new constraints, and would need to be applied against the pin connection rotation direction, as well across the pin connection rotation direction.

The design buckling load for column members was calculated as per AS4100 standards, using Equation 18 from Section 2.4.2.4;

$$N_{om} = \frac{\pi^2 EI}{(k_e l)^2}$$

where

N_{om} = elastic buckling load of a member
E = Young's modulus
I = cross-sectional moment of area of a member
k_e = member effective length factor given by Figure 2.12.
l = member length

The design buckling load calculated for the original structure was determined to be 480 kN, and the design buckling load calculated for the alternative structures was determined to be 235 kN, using the same circular hollow section in the column members (refer to Appendix D for calculations). The design buckling load for the alternative tower structures is almost half of that for the original structure, hence care needs to be taken when comparing analysis solutions to the benchmark of design developed from the comparative analysis. Therefore, it would be pertinent for the benchmark of design to be adjusted to account for the changes in design criteria.

An additional change that was proposed to the original structure was to use steel wire rope as supporting tensile guy wires, which were to be applied with either external or internal anchoring, as shown by Figure 3.8. Analysis on guy wires were conducted in combination with the static structural loading analysis, using FE simulations in ANSYS Workbench. The following approach was used in the simple design and selection of externally anchored guy wires, and a similar approach was used in the design of the winch cable used in the tilt-up tower:

- The guy radius x_{guy} between wire ground anchor and tower anchor was specified.
- The preliminary wire breaking force F_T in the guy wire was calculated using a simple 2D truss analysis conducted on the guyed structure under wind loading (refer to Figure 3.9).
- A preliminary wire rope diameter was selected from AS3569 tables of minimum breaking force according to the required breaking force.
- FE simulations were conducted on the preliminary configuration.
- x_{guy} and wire rope diameter were adjusted until an optimal wire designation was selected.

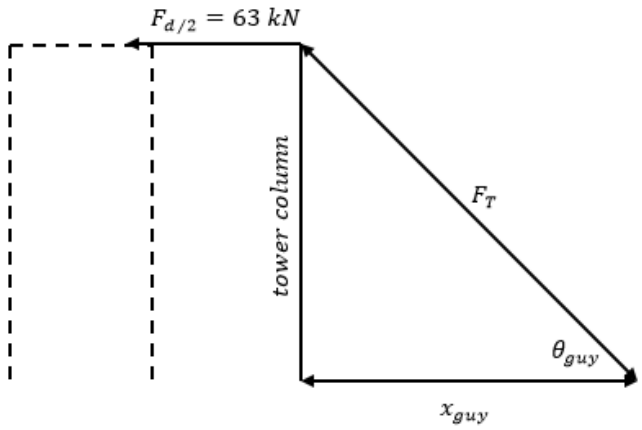

Figure 3.9: Schematic of Preliminary Guy Wire Tensile Load

The optimal wire would then be used in final static structural loading analysis of both externally, and internally guyed structures. Therefore, an additional design benchmark would need to be facilitated, specifically for the design breaking strain for guy wires used for cooling towers within the scope of this thesis. Refer to Appendix E for preliminary wire breaking force calculations.

4 SIMULATION MODELS

This chapter will present the models used to conduct structural FE analysis and simulations, and shall detail the construction of geometries, key dimensions, and the application of boundary conditions used to obtain results. All FE simulations were conducted using ANSYS Workbench. For definitions of terms used in ANSY Workbench for simulations, refer to the ANSYS DesignModeler User's Guide [27], and ANSYS Mechanical User's Guide [26].

4.1 Validation Model

The validation model was used in a comparative study to replicate and ascertain what assumptions were made in a previous analysis on the QGECE Hybrid Cooling Tower.

4.1.1 Geometry

The geometry replicated from the previous analysis in the validation model consisted of the following elements:

- Line bodies for each structural member, with cross-sections as follows;
  - 1 × 323.9 × 9.5 mm CHS top ring beam.
  - 4 × pairs of 273.1× 6.4 mm CHS V – columns.
- Overall dimensions:
  - Height: 20,000 mm.
  - Ring beam diameter: 12,525 mm.
  - Column footing diameter: 13,990 mm.

The geometry of the validation model construction in ANSYS DesignModeler is shown in Figure 4.1.

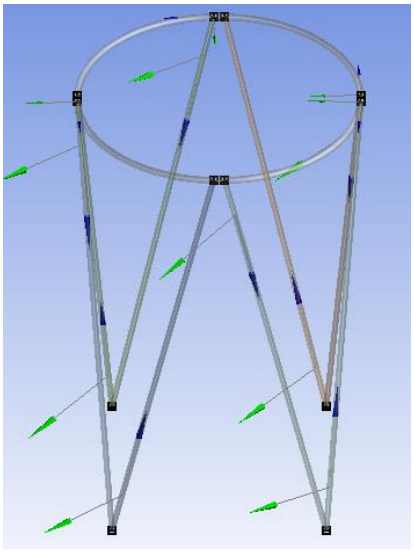

Figure 4.1: Validation Model Geometry

4.1.2 Boundary Conditions

The following boundary conditions were replicated from the previous analysis in the validation model:

- Axial force acting downward simulating membrane and ring beam self-weight (applied as 40 kN force, refer Figure 4.2).
- Wind loading as point loads, and a distributed load applied at 0° wind orthogonal directions (applied as 450 N/m line pressures, refer Figure 4.3).
- Wind loading as point loads, and a distributed load applied at 45° wind orthogonal directions (applied as 450 N/m line pressure, refer Figure 4.4).
- A combination of the axial and point loads, and axial and distributed loads, applied at 0° and 45° wind orthogonal directions.
- Stand earth gravity.
- Fixed Ground Supports.

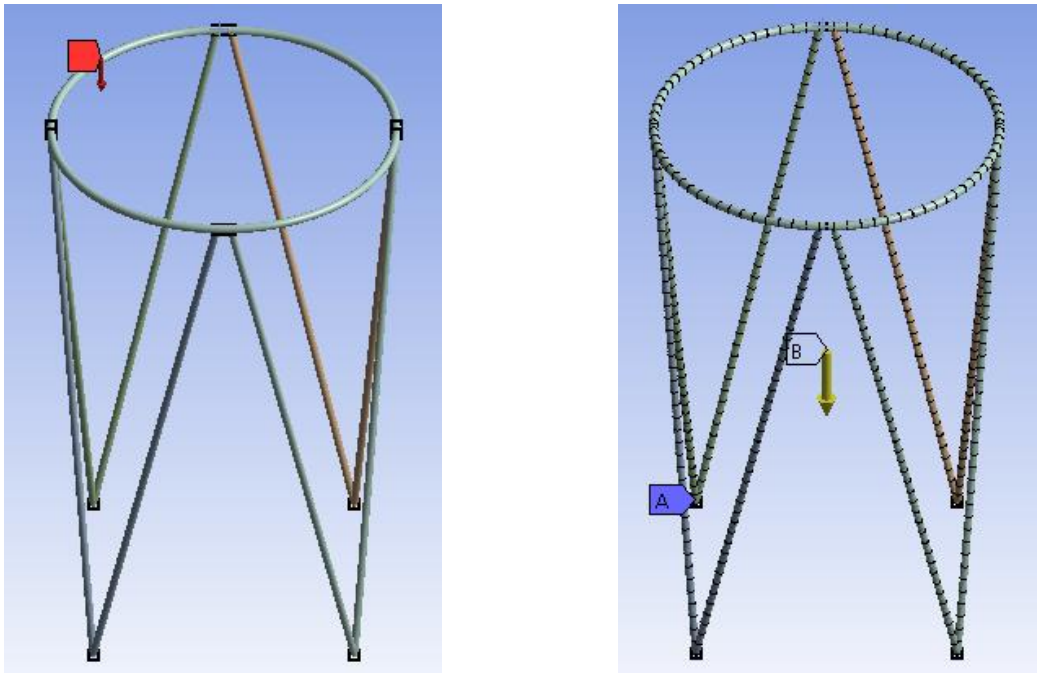

Axial Load **Mesh and Other Boundary Conditions**

Figure 4.2: Validation Model Boundary Conditions

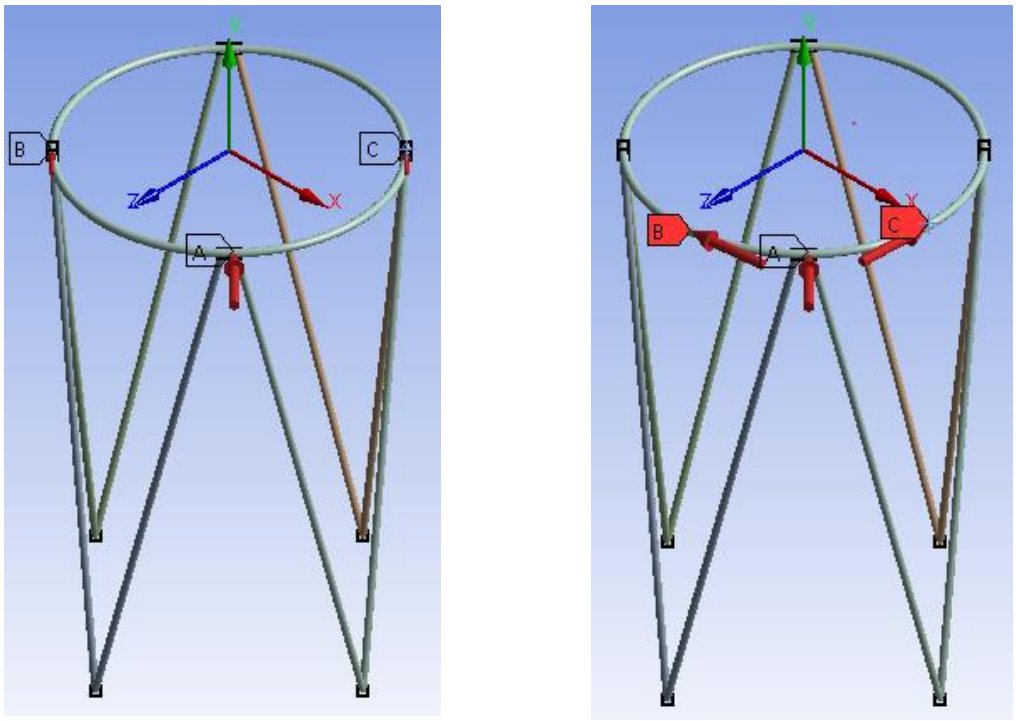

Point Load **Distributed Load**

Figure 4.3: Validation Model Boundary Conditions - 0° Orthogonal Direction

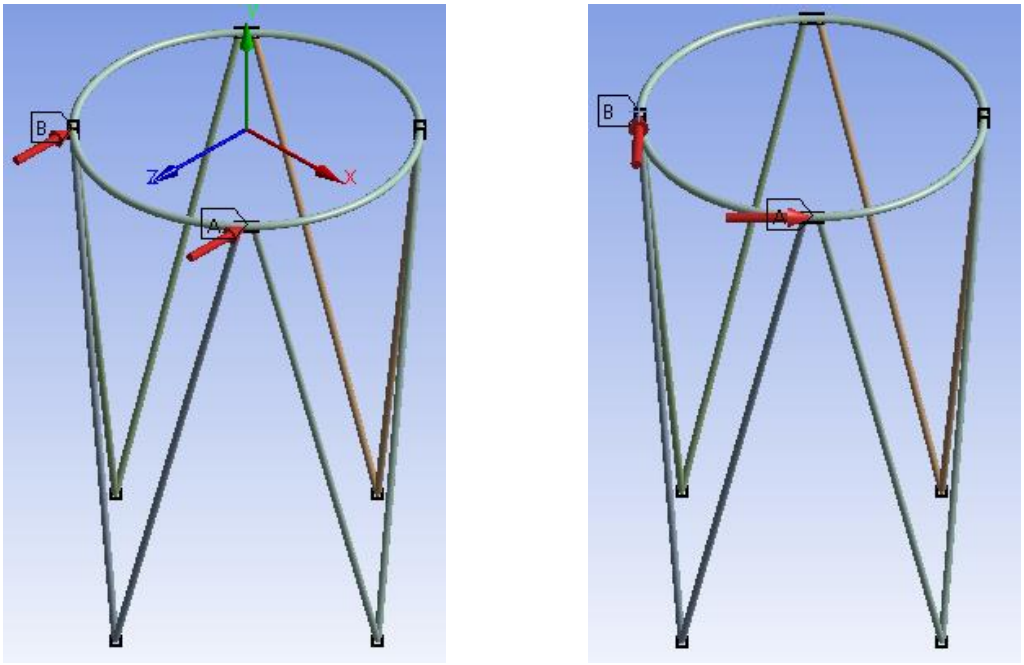

Point Load **Distributed Load**

Figure 4.4: Validation Model Boundary Conditions - 45° Orthogonal Direction

The geometries and boundary conditions were replicated as closely as possible to that of the previous analysis. However, without explicit detail of the geometry and boundary conditions used in the previous analysis it is difficult to create a wholly certain replication.

4.2 Benchmark Model

The benchmark model was used in a benchmark analysis to develop a benchmark of design, which would be used to compare against alternative designs developed throughout the thesis.

4.2.1 Geometry

The geometry of the benchmark model consisted of the following elements:

- Line bodies for each structural member, with cross-sections as follows;
  - 1 × 323.9 × 9.5 mm CHS top ring beam.
  - 1 × 323.9 × 9.5 mm CHS bottom ring beam
  - 4 × pairs of 273.1× 6.4 mm CHS V – columns.
- Overall dimensions:
  - Height: 20,000 mm.
  - Distance between top and bottom ring beams: 15,000 mm.
  - Ring beam diameter: 12,525 mm.
  - Column footing diameter: 13,990 mm.

Figure 4.5 and Figure 4.6 display the benchmark model geometry constructed in ANSYS DesignModeler for 0° and 45° building orthogonal directions respectively, and are shown with vertices displayed.

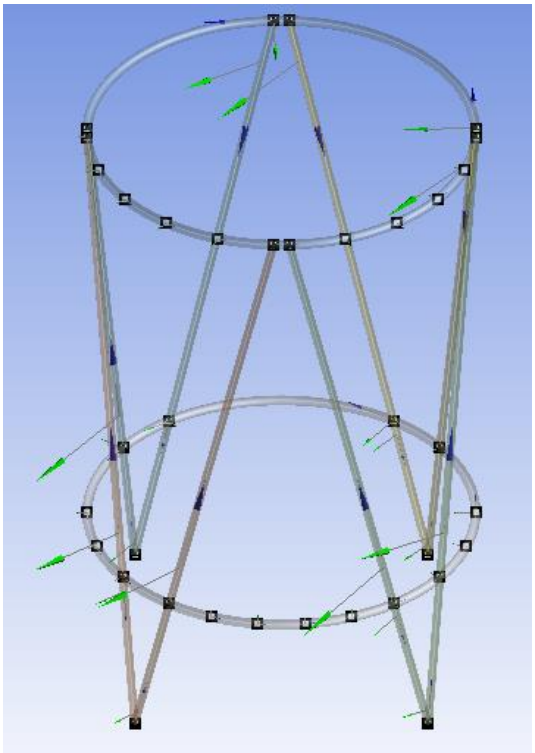

Figure 4.5: Benchmark Model Geometry - 0° Orthogonal Direction

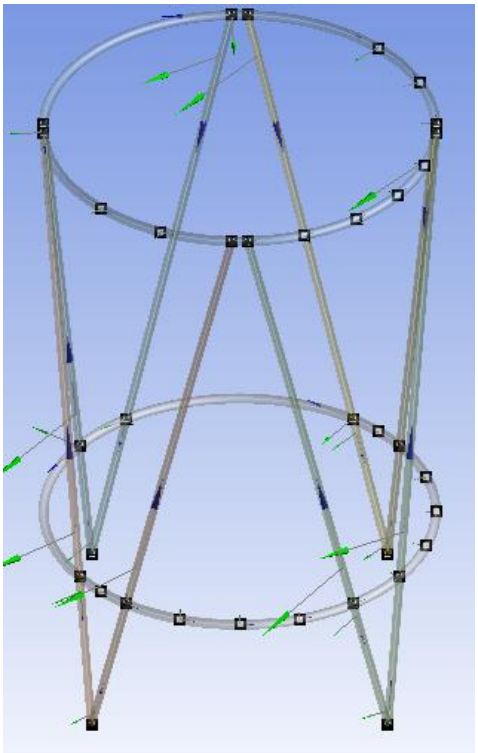

Figure 4.6: Benchmark Model Geometry - 45° Orthogonal Direction

4.2.2 Boundary Conditions

The boundary conditions applied to the benchmark model included the following, and are shown in Figure 4.7 and Figure 4.8, for 0° and 45° building orthogonal directions respectively:

- Membrane pretension (applied as 3000 N/m line pressure).
- Wind loading (applied using the circumferential load distribution defined in Section 3.3 using line pressures as per geometry in Figure 4.5, Figure 4.6)
- Standard earth gravity.
- Fixed ground supports.

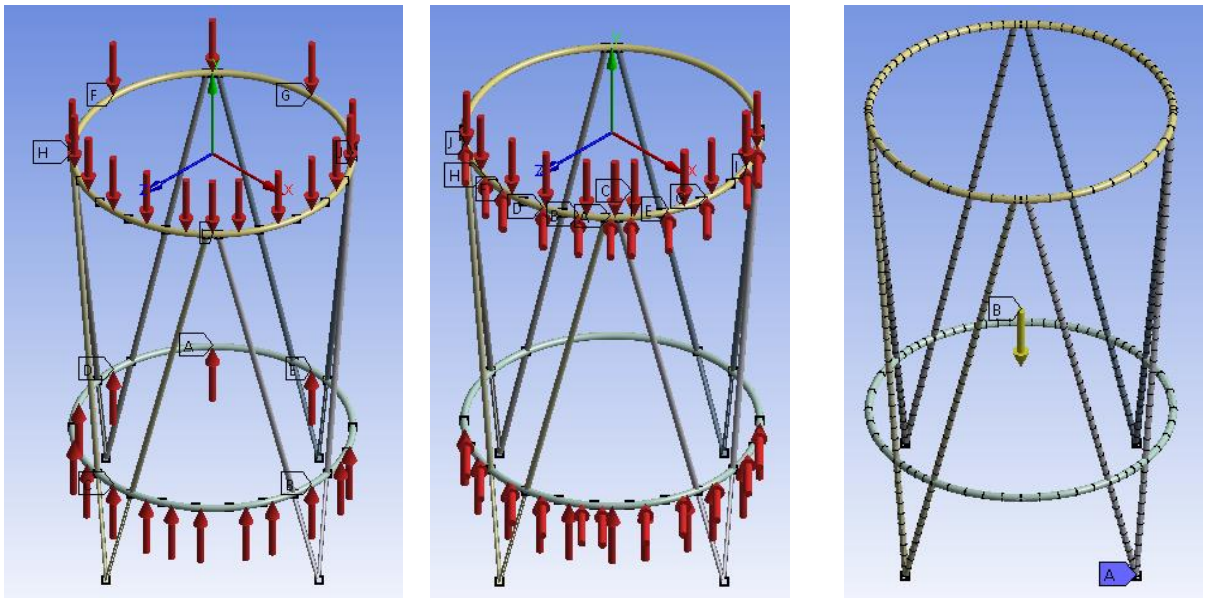

Membrane Pretension **Wind Loading** **Mesh and Other Boundary Conditions**

Figure 4.7: Benchmark Model Boundary Conditions - 0° Orthogonal Direction

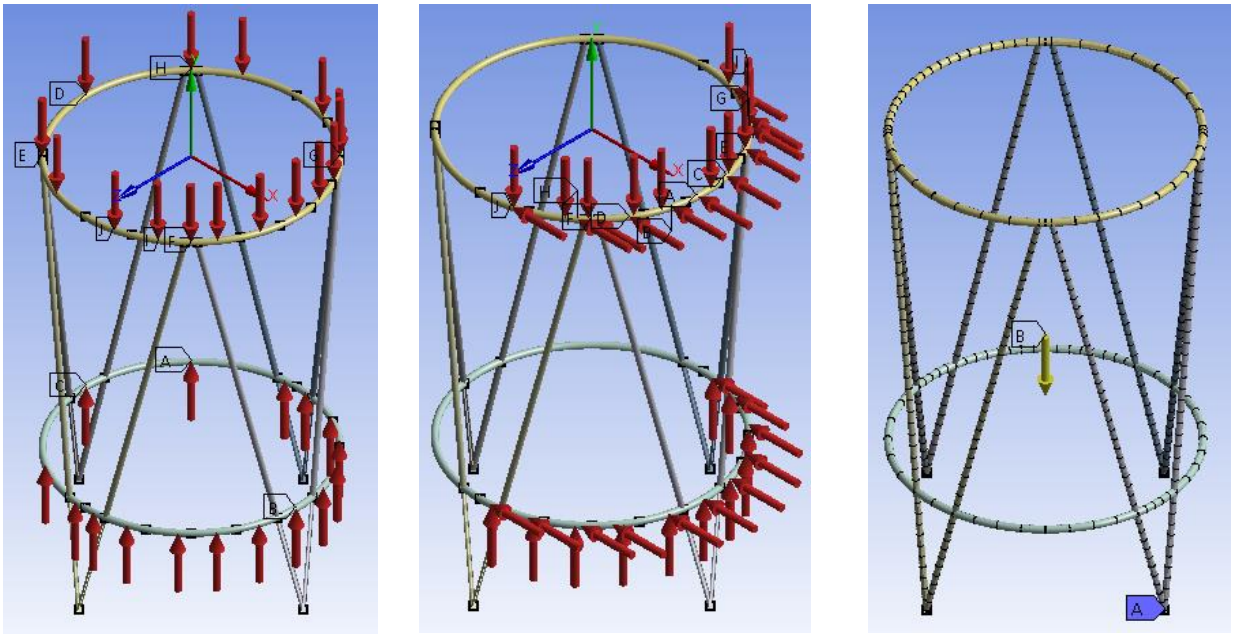

Membrane Pretension **Wind Loading** **Mesh and Other Boundary Conditions**

Figure 4.8: Benchmark Model Boundary Conditions - 45° Orthogonal Direction

4.3 Tilt-Up Tower Models

The tilt-up tower models were used to analyse the feasibility of the tilt-up tower method, and to validate rudimentary hand calculations. Simulation models were altered and analysed iteratively until an optimal solution was achieved.

4.3.1 Geometry

The geometry of the tilt-up tower models were analysed with and without a gin pole, and at erection height intervals, 5 m, 10 m, and 15 m. The geometry consisted of the following elements:

- Line bodies for each structural member, with cross-sections as follows;
    - 1 × 323.9 × 9.5 mm CHS top ring beam (initial iteration).
    - 1 × 323.9 × 12.7 mm CHS top ring beam (final iteration).
    - 4 × 273.1 × 6.4 mm CHS columns.
    - 1 × 273.1 × 6.4 mm CHS gin pole.
    - 1 × 40 mm diameter cable members (initial iteration).
    - 1 × 13 mm diameter cable members (final iteration).
- Overall dimensions:
    - Height: 20,000 mm.
    - Column length: 20,000 mm.
    - Ring beam diameter: 12,525 mm.
    - Column footing diameter: 12,525 mm.
    - Horizontal winch distance, $x_{winch,max}$: 20,000 mm.
    - Gin pole length, L_{gin}: 15,000 mm.
    - Gin pole angle θ_{gin}: 90°

Figure 4.9 and Figure 4.10 show the geometry constructed in ANSYS DesignModeler for the tilt-up tower without and with a gin pole respectively, for erection heights of 5 m, 10 m, and 15 m.

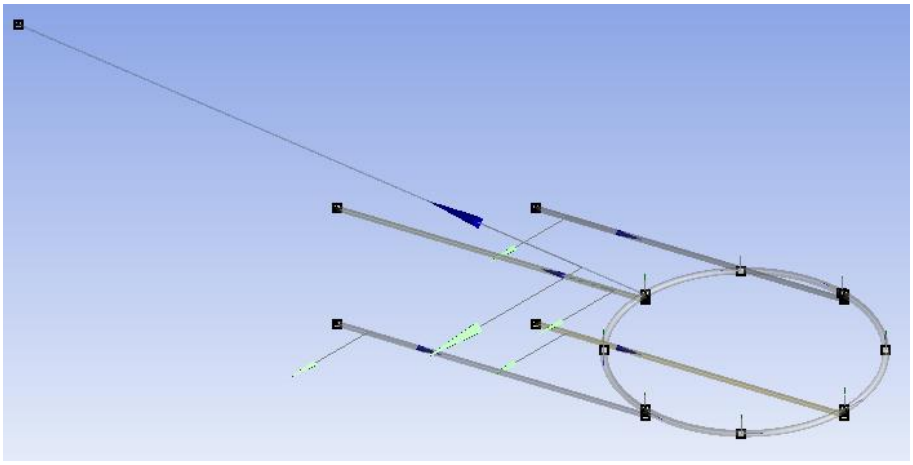

Erection Height – 5 m

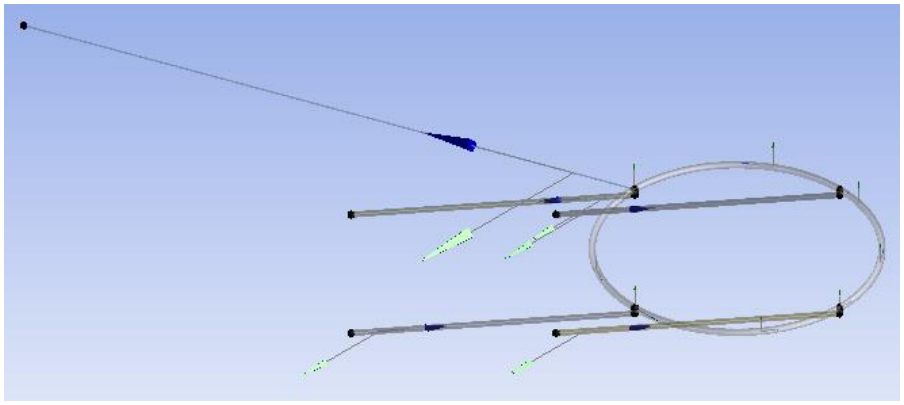

Erection Height – 10 m

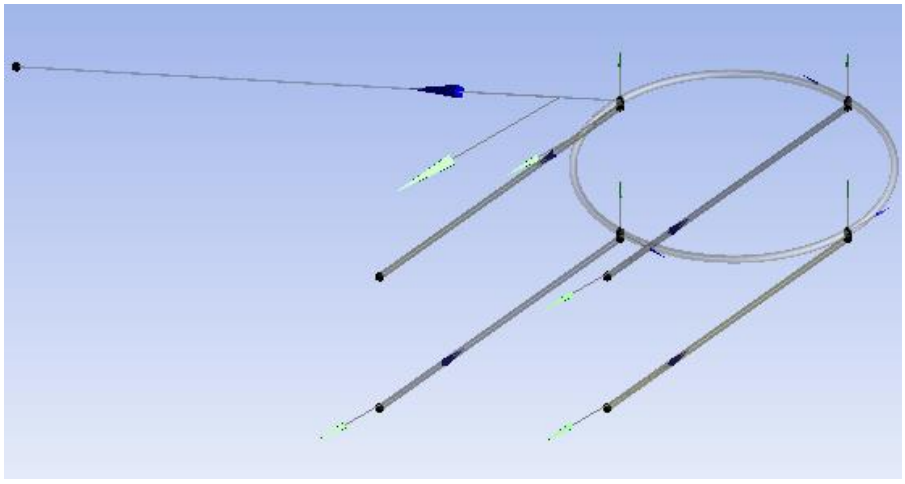

Erection Height – 15 m

Figure 4.9: Tilt-Up Tower Model Geometry – without Gin Pole

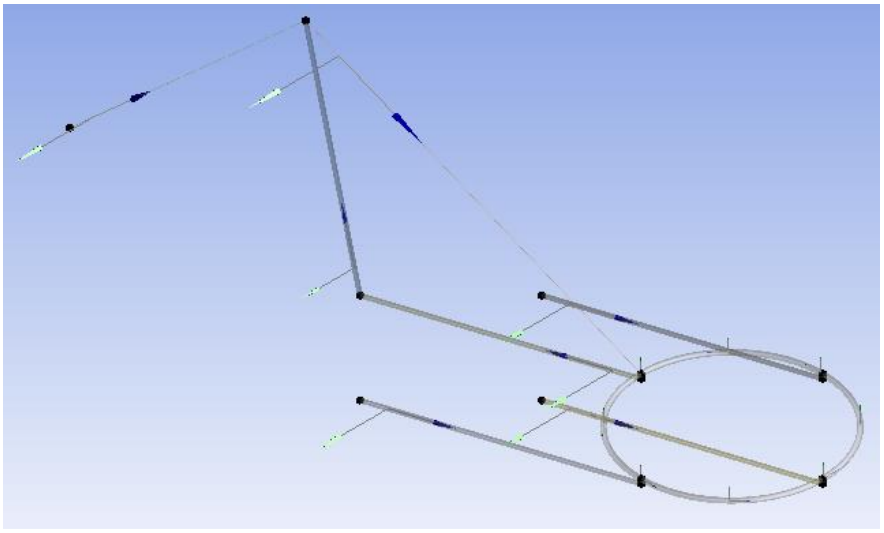

Erection Height – 5 m

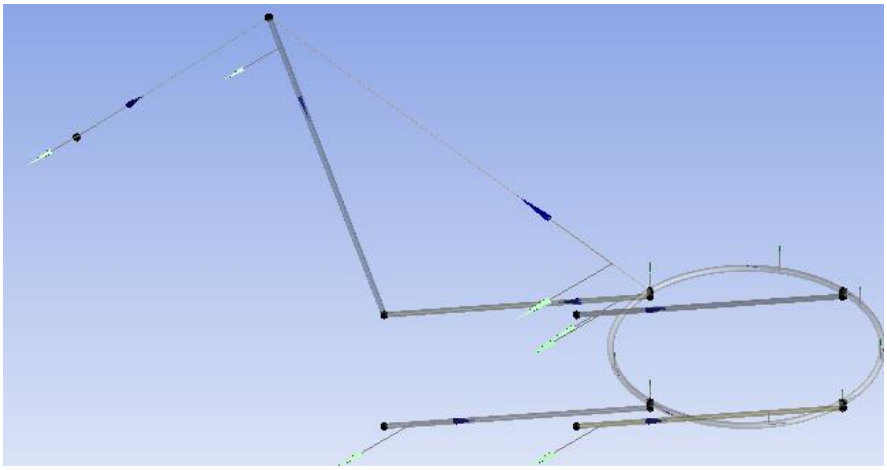

Erection Height – 10 m

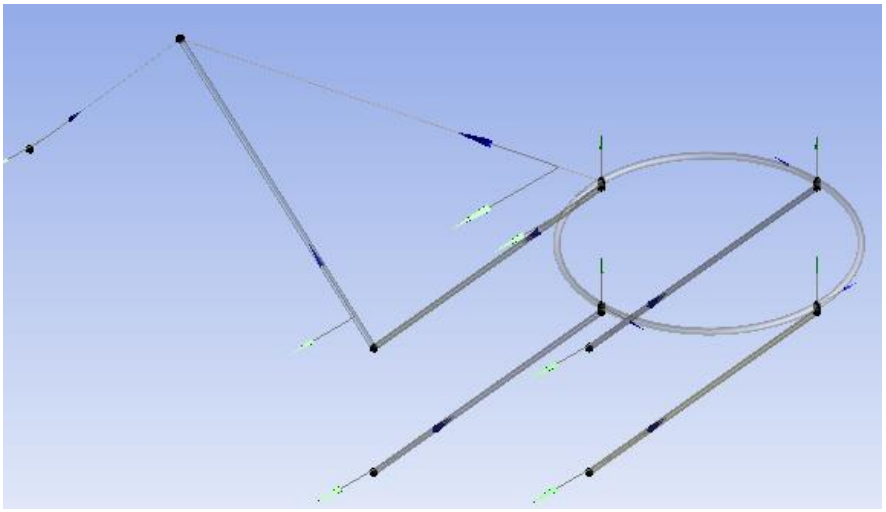

Erection Height – 15 m

Figure 4.10: Tilt-Up Tower Model Geometry – with Gin Pole

4.3.2 Boundary Conditions

The boundary conditions and connections applied to the tilt-up tower models included the following, and are shown in Figure 4.11 and Figure 4.12, for towers without and with a gin pole respectively:

- Revolute – ground to line body connections for column feet.
- Fixed – ground to line body connections for cable members.
- Fixed – line body to line body connections for cable member to ring/column joints.
- Fixed – line body to line body connections for gin pole to column joints.
- End release – rotation axis Z free connections for column to ring joints.
- End release – rotation axis Z free connections for gin pole to cable member joints.
- Standard earth gravity.

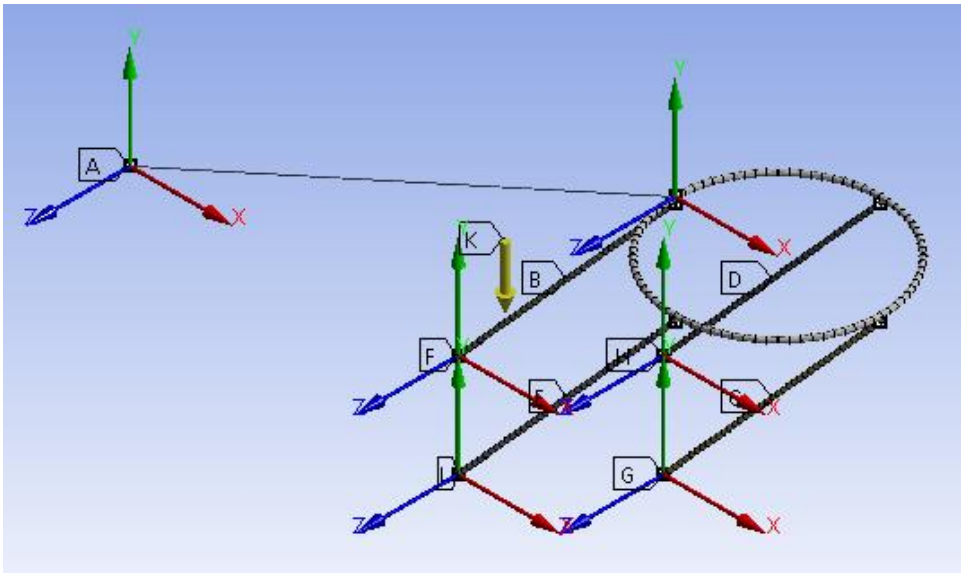

Figure 4.11: Tilt-Up Tower Model Boundary Conditions – without Gin Pole

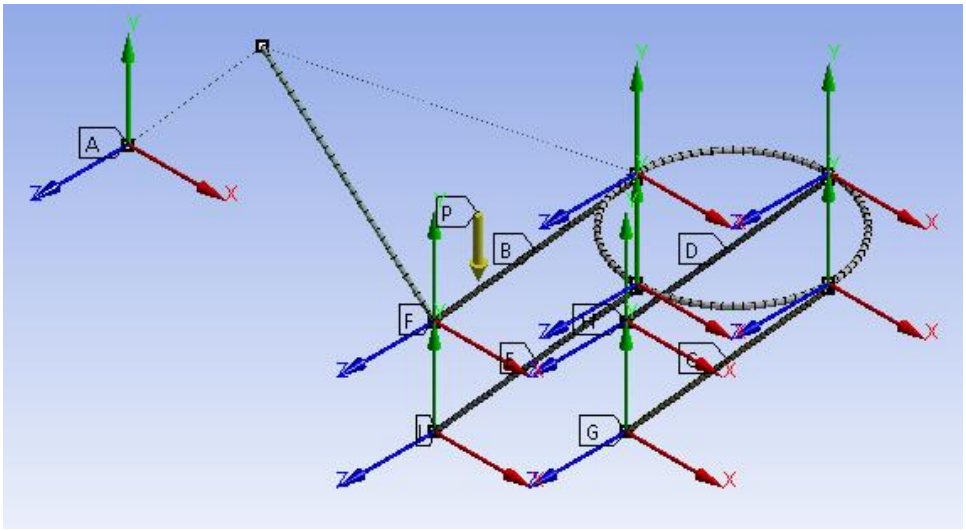

Figure 4.12: Tilt-Up Tower Model Boundary Conditions – with Gin Pole

4.4 Alternative Geometry Models

The alternative geometry models were used to analyse the alternative cooling tower structural geometries introduced in Section 3.6.2. Simulation models were altered and analysed iteratively until an optimal solution was achieved.

4.4.1 Geometry

The geometry of the alternative geometry models were analysed with guy wires being anchored externally (Alternative A), and internally (Alternative B). The geometry consisted of the following elements:

- For Alternative A; line bodies for each structural member with cross-sections as follows;
    - 1 × 323.9 × 9.5 mm CHS top ring beam (initial iteration).
    - 1 × 323.9 × 12.7 mm CHS top ring beam (final iteration).
    - 4 × 273.1 × 6.4 mm CHS columns (initial iteration).
    - 4 × 323.9 × 9.5 mm CHS columns (final iteration).
    - 4 × 12 mm cable members (initial iteration).
    - 4 × 22 mm cable members (final iteration).
- For Alternative B:
    - 1 × 323.9 × 9.5 mm CHS top ring beam (initial iteration).
    - 1 × 323.9 × 12.7 mm CHS top ring beam (final iteration).
    - 4 × 273.1 × 6.4 mm CHS columns.
    - 8 × 12 mm cable members (initial iteration).
- Overall dimensions for both alternatives:
    - Height: 20,000 mm.
    - Column length: 20,000 mm.
    - Ring beam diameter: 12,525 mm.
    - Column footing diameter: 12,525 mm.
    - Guy Radius (Alternative A):
        - 12,000 mm (initial iteration).
        - 20,000 mm (final iteration).

Figure 4.13 and Figure 4.14 show the geometry constructed in ANSYS DesignModeler for Alternative A and Alternative B respectively, and are shown with vertices displayed.

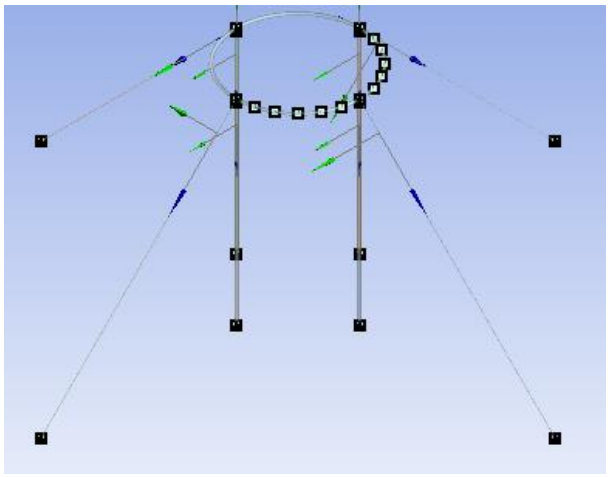

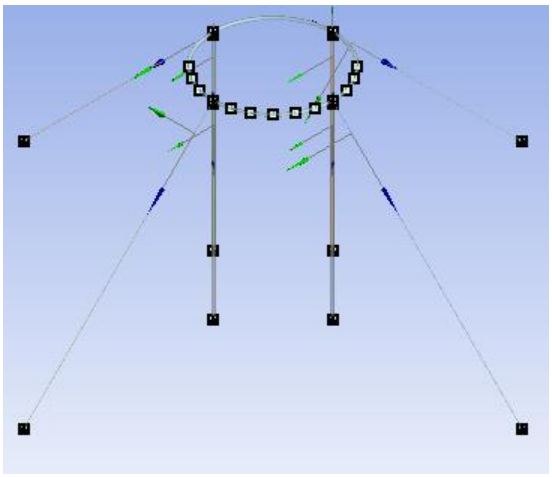

0° Orthogonal Direction **45° Orthogonal Direction**

Figure 4.13: Alternative A Model Geometry

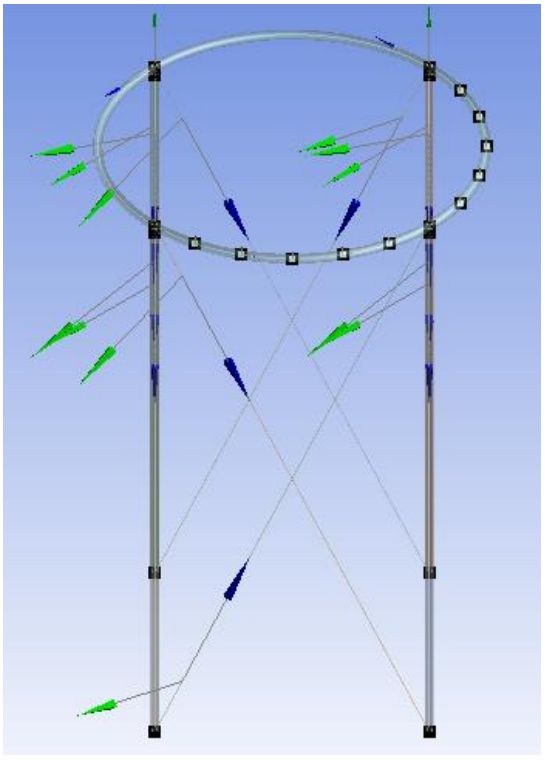

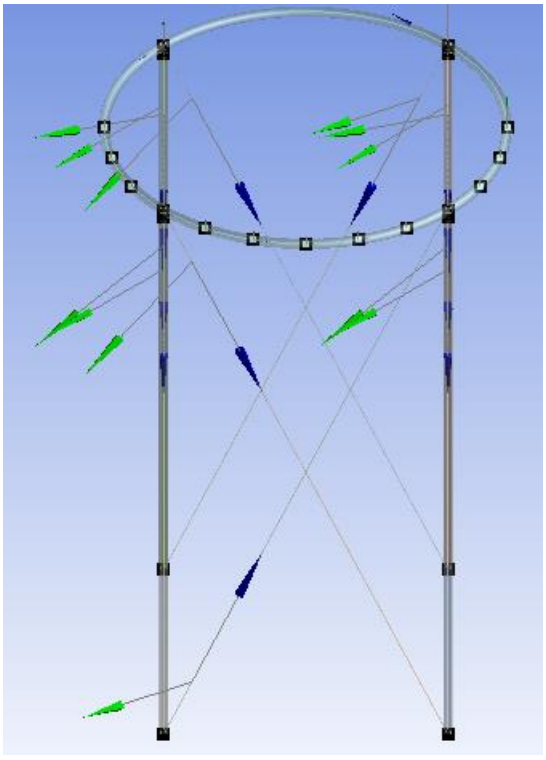

0° Orthogonal Direction **45° Orthogonal Direction**

Figure 4.14: Alternative B Model Geometry

4.4.2 Boundary Conditions

The boundary conditions and connections applied to the alternative geometry models included the following, and are shown in Figure 4.15 and Figure 4.16 for Alternative A for 0° and 45° orthogonal directions respectively. Alternative B is shown in Figure 4.17 and Figure 4.18 for 0° and 45° orthogonal directions respectively:

- For Alternative A:
    - Revolute – ground to line body connections for column feet.
    - Fixed – ground to line body connections for guy wire members.
    - Fixed – line body to line body connections for guy wire member to ring/column joints.
    - End release – rotation axis Z free connections for column to ring joints.
    - Membrane pretension (applied as 3000 N/m line pressure).
    - Wind loading applied at 0° and 45° orthogonal directions (applied using the circumferential load distribution defined in Section 3.3 using line pressures as per geometry in)
    - Standard earth gravity.
- For Alternative B:
    - Revolute – ground to line body connections for column feet.
    - Fixed – line body to line body connections for guy wire member to ring/column joints.
    - End release – rotation axis Z free connections for column to ring joints.
    - Membrane pretension (applied as 3000 N/m line pressure).
    - Wind loading applied at 0° and 45° orthogonal directions (applied using the circumferential load distribution defined in Section 3.3 using line pressures as per geometry in)
    - Standard earth gravity.

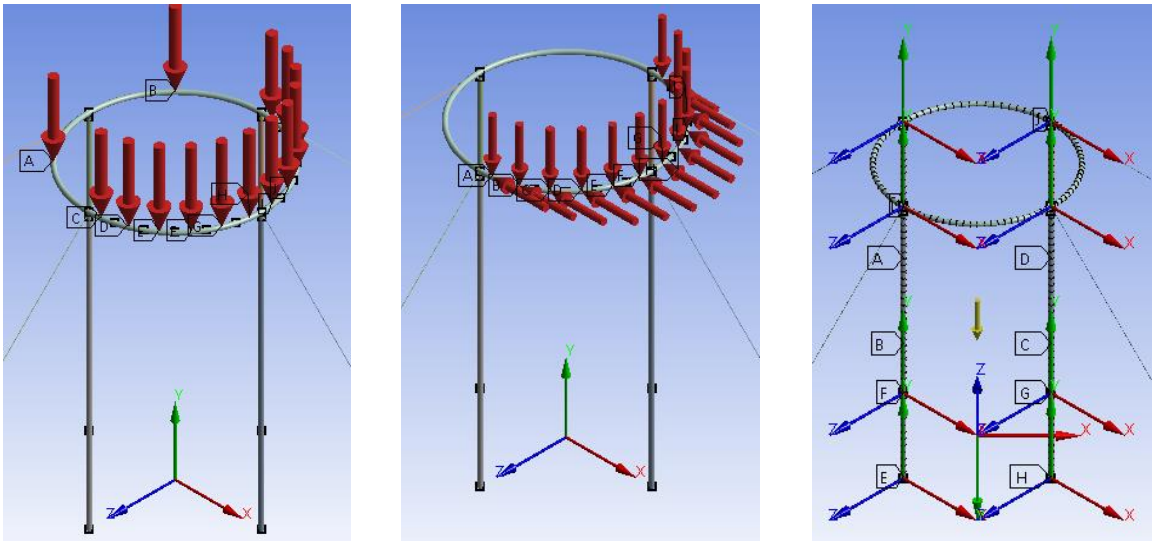

Membrane Pretension **Wind Loading** **Connections, Mesh & Other Loads**

Figure 4.15: Alternative A Model Boundary Conditions - 0° Orthogonal Direction

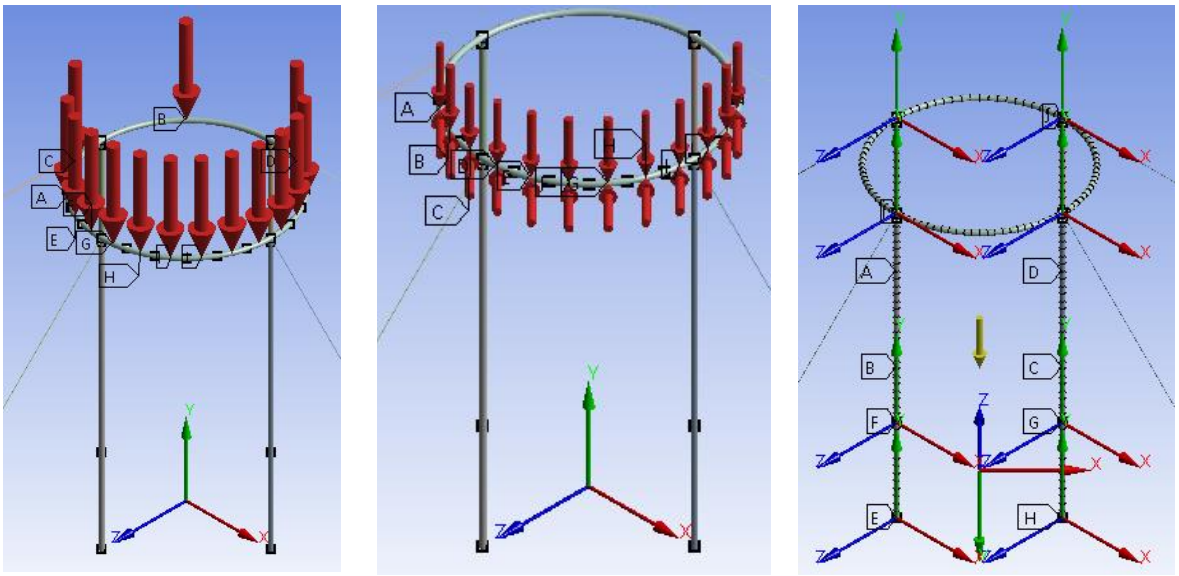

Membrane Pretension **Wind Loading** **Connections, Mesh & Other Loads**

Figure 4.16: Alternative A Model Boundary Conditions - 45° Orthogonal Direction

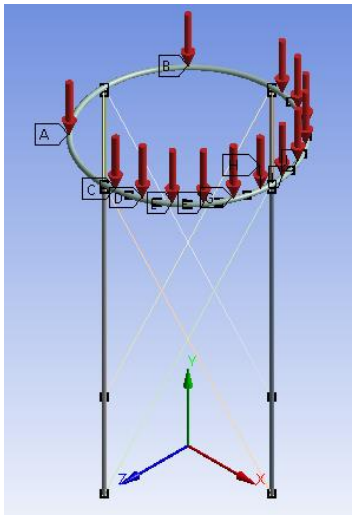

Membrane Pretension

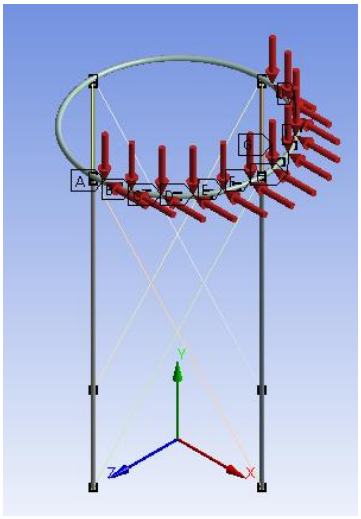

Wind Loading

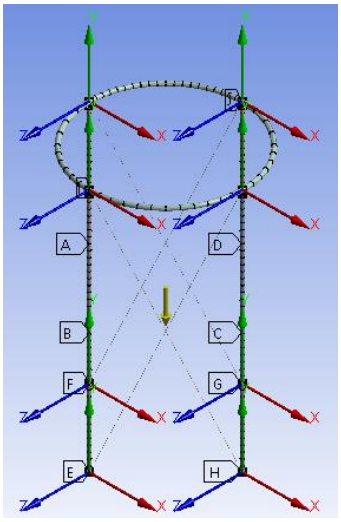

Connections, Mesh & Other Loads

Figure 4.17: Alternative B Model Boundary Conditions - 0° Orthogonal Direction

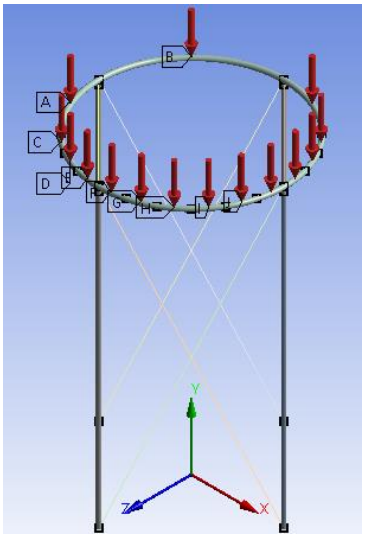

Membrane Pretension

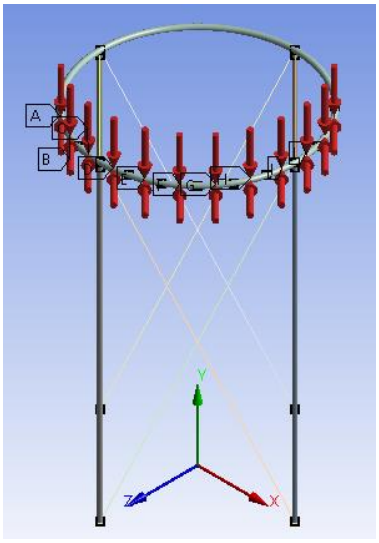

Wind Loading

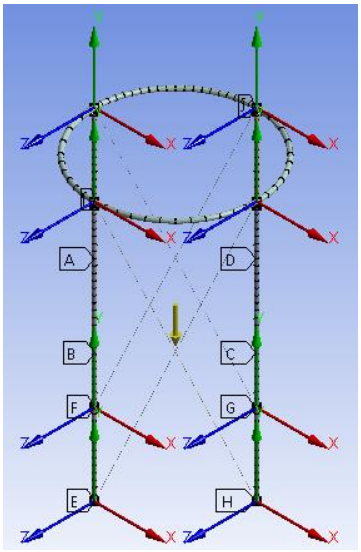

Connections, Mesh & Other Loads

Figure 4.18: Alternative B Model Boundary Conditions - 45° Orthogonal Direction

5 RESULTS AND DISCUSSION

The following chapter shall present an in-depth analysis and discussion of results, including analysis and discussion of; FE simulation results, analytical calculation results, as well as presenting the benchmark of design and limiting factors for cooling towers within the scope of this thesis.

5.1 Validation Analysis

The convergence results of the validation analysis, following the approach presented in Section 3.4, are shown in Table 5.1.

Table 5.1: FEA Results of Previous Analysis Compared to Validation Analysis

FE Analysis	Wind Orthogonal Direction	$\sigma_{combined}$ (MPa)
Previous Analysis	0°	23
	45°	21
Validation Analysis	0°	22
	45°	22

The results in Table 5.1 showed that the validation analysis was able to obtain results which converged to within 5% of that of the previous analysis. However, in validating the analysis some oversights in the model were discovered. The most significant of the oversights were the omission of the bottom ring beam, the inclusion of gravity as a boundary condition, which was not explicitly stated in the previous analysis, and the assumptions made about wind loading on the cooling tower, as well as other significant loads, such as pretension of the PVC membrane.

It was concluded from the comparative study that the discrepancy in the results between the models was largely due to these oversights. The conclusion made about these oversights are somewhat subjective, regardless of the presence of comparative data. Without exact details regarding the assumptions and boundary conditions used in the previous analysis, and without being able to view to model used for what it was, it is difficult to be purely objective as to the reason for these discrepancies.

Regardless, by accounting for the oversights concluded from the comparative study, and by conducting additional FE analysis in accordance to relevant standards, a benchmark of design and several limiting factors were developed, which would be used to compare against alternative designs developed throughout the thesis.

5.2 Benchmark of Design

The results from the benchmark analysis as a result of the comparative study shown in Sections 3.4 and 5.1 are shown in Table 5.2. The following criteria were defined to analyse the performance of the benchmark analysis.

- F_{axial}: the maximum compressive (or tensile) axial load in any column.
- $\sigma_{bending}$ (columns): the maximum bending stress present in any column.
- $\sigma_{bending}$ (rings): the maximum bending stress present in any ring beam.
- $\delta_{Total:}$ the maximum total horizontal deflection at any point of the structure.
- $F_{reaction\ horizontal:}$ the total reaction force at ground supports, which was used to validate FE results, and should have a solution close to that of the total wind force.

Table 5.2: Benchmark Analysis Results

	Wind Orthogonal Direction	
Criteria	0°	45°
F_{axial} columns (kN)	122	113
$\sigma_{bending}$ columns (MPa)	76	88
$\sigma_{bending}$ rings (MPa)	129	124
δ_{Total} (mm)	44	35
$F_{reaction\ horizontal}$ (kN)	134	134

The difference between results for the total reaction force at ground supports in the FE analysis, and the total wind load determined analytically was approximately 4%. It was concluded that the difference in these results was due to assumptions made when calculating the analytical wind force, compared to assumptions FE models use when computing simulation results.

The QGECE Hybrid Cooling Tower has been in service for over 12 months without reported failure; hence, it may be assumed that results from the benchmark analysis may be used as a benchmark of design. Because of the changes made to the original structure in order to accommodate the tilt-up method, some design criteria were redefined. Maximum bending stress in the columns, and the total horizontal reaction forces were omitted from the benchmark of design, as the columns will fail in buckling, and the reaction force was used strictly for the purpose of validating the FE model solutions. Criteria for wire breaking force, and gin pole buckling load were also added. Therefore, Table 5.3 was defined as the benchmark of design for cooling towers within the scope of this thesis.

It is important to note that the criteria set by the validation analysis results are calculated from a previous analysis and are used to compare design values to indicate trends in analysis results. The criteria set by the benchmark of design are the maximum permissible design value, and should not be exceeded, to ensure the component associated with the criteria does not fail. If the maximum permissible design value, or the limiting factor, is exceeded, that particular component/criteria should be redesigned and re-evaluated until a safe solution is obtained.

Table 5.3: Cooling Tower Benchmark of Design

Criteria	Limiting Factor
Column Buckling Load (kN)	235
Ring Bending Stress (MPa)	129
Horizontal Deflection (mm)	44
Wire Breaking Force (kN)	≤ specified wire breaking force
Gin Pole Buckling Load (kN)	573

5.3 Tilt-Up Tower Feasibility

The results from the feasibility analysis conducted to determine if a tilt-up tower would be appropriate, as outlined in Section 3.6.1, have been presented in the following section. Figure 5.1 presents the comparison of the maximum axial force for any part of the tower structure as a function of the erection height, for the tilt-up method with and without the aid of a gin pole. It is evident that without the support of a gin pole, the maximum axial force, which was found in the winch cable, was impractically large at lower erection heights. The results were obtained for a maximum horizontal winch distance $x_{winch,max}$ of 20 m.

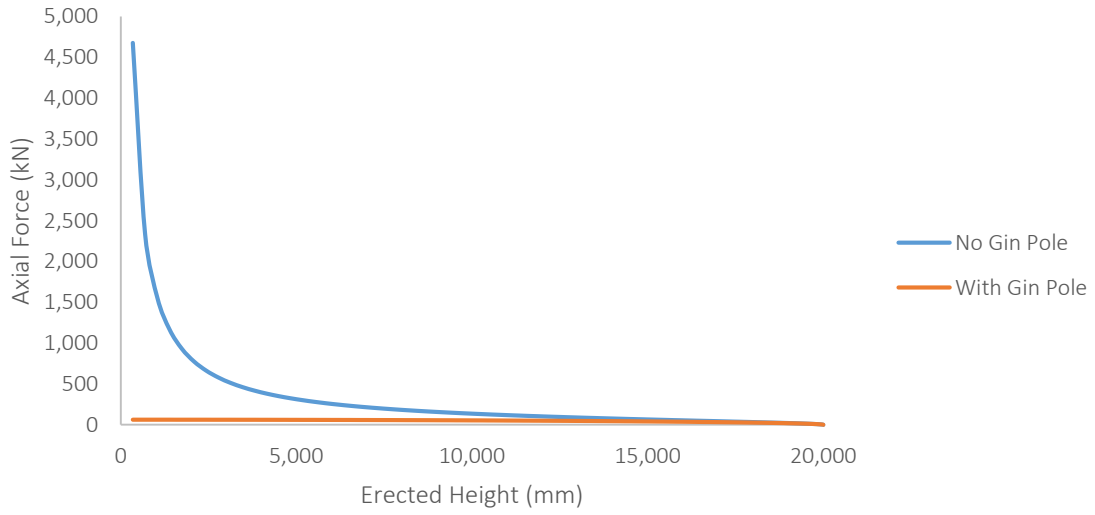

Figure 5.1: Tilt-Up Tower Analytical Results – Winch Cable Force

However, with the addition of a gin pole, as shown clearer in Figure 5.2, the maximum axial force was dramatically reduced throughout all stages of erection.

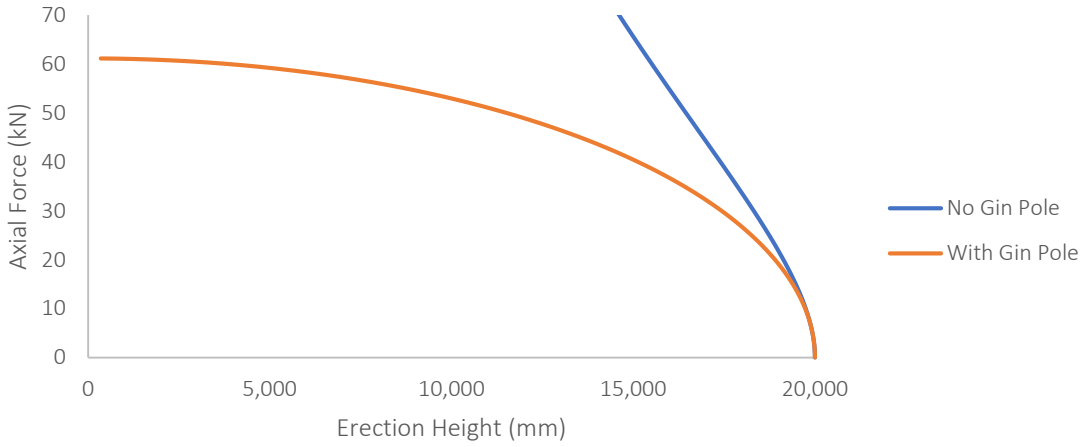

Figure 5.2: Tilt-Up Tower Analytical Results – Winch Cable Force with Gin Pole

These results were obtained using a gin pole length L_{gin} of 15 m and a gin pole angle θ_{gin} of 90°. With these gin pole parameters, it was observed that the analytical results for maximum axial force, with and without the aid of the gin pole, converged at greater erection heights. This observation may suggest that at particular erection angles and consequent erection heights, and depending on the parameters of the gin pole, the gin pole may eventually become inactive.

The parameters for the gin pole were also adjusted to observe what effects altering parameters had on the analytic results. The following observations were made for the given parameter adjustments:

- Increasing/decreasing gin pole length, L_{gin}: reduces/increases maximum axial force.
- Increasing/decreasing gin pole angle θ_{gin}: increases/reduces maximum axial force.
- Increasing/decreasing maximum horizontal winch distance $x_{winch,max}$: reduces/increases maximum axial force without gin pole (does not affect gin pole results).

FE simulations were conducted on a selection of erection heights throughout the erection procedure for tilt-up towers with and without the aid of a gin pole. The results of these FE simulations in terms of the benchmark of design, as well as the winch cable force and gin pole, are shown in Figure 5.3. The results shown are for a winch cable with diameter of 40 mm, which was initially chosen for being the most simple wire class type with the highest minimum breaking force, which was specified as 1040 kN for a Grade 1960 Class 6 × 7 with fibre core (refer to AS3569).

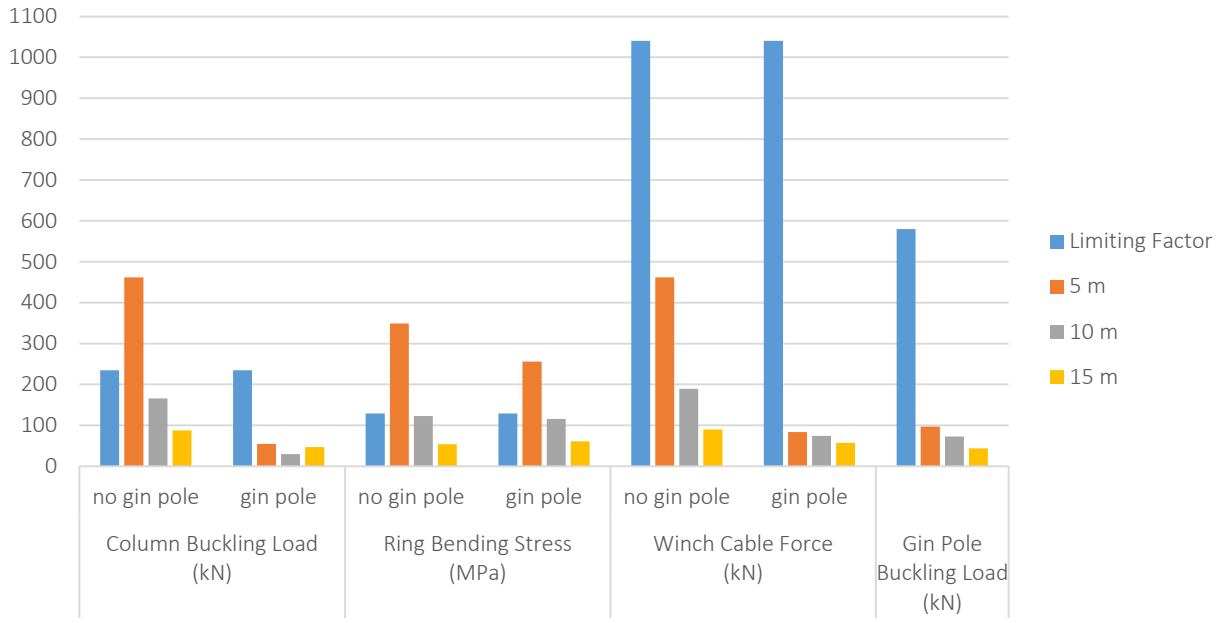

Figure 5.3: Tilt-Up Tower FE Simulation Results

It is evident from the FE simulation results that the use of a gin pole significantly reduced the maximum result for the specified criteria. In comparison to the benchmark of design, the results for the various stages of the erection heights shown, meet the limiting factor, except for the ring bending stress at 5 m, the results for which will be discussed later in this section.

A comparison was also made between the FE simulation results and analytical results for maximum axial force in the structure, to determine how well the analytical results validate the FE results, as shown in Figure 5.4.

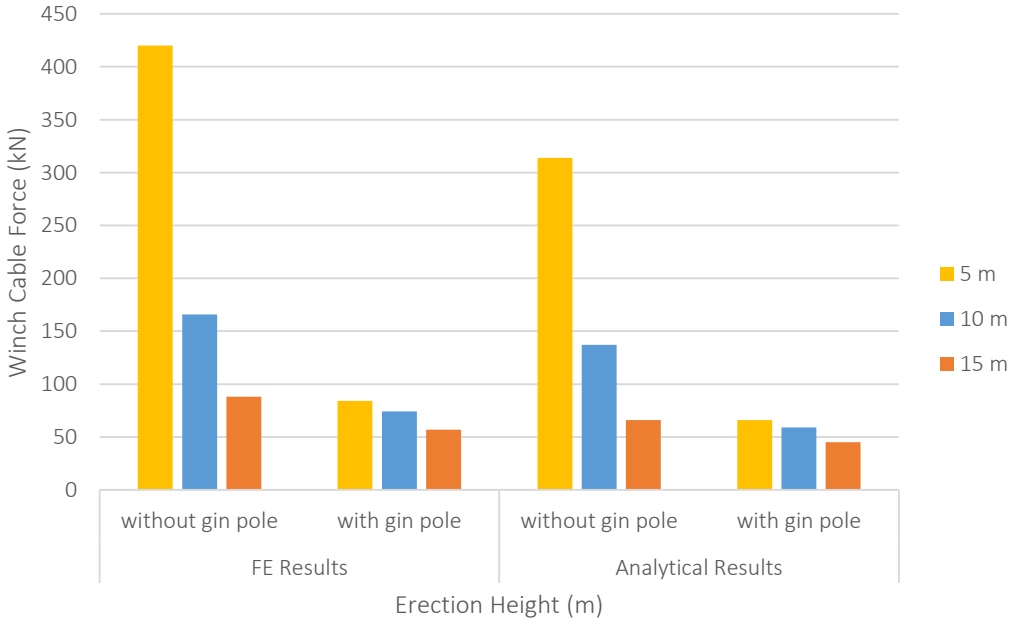

Figure 5.4: Tilt-Up Tower FE Simulation and Analytical Result Comparison

Evidently, there were marginally clear discrepancies between FE simulation results and analytical results. The reason for these discrepancies were deduced to be due to the 2D truss analysis's failure to account for the effects of sag in the winch cable that is taken up due to the self-weight of the structure under gravity. Additionally, the more complicated geometry of the top ring beam would behave much differently than when analysed as a simple 2D truss, hence the axial and nodal forces determined analytically were not entirely indicative of that of the true geometry.

Given that the maximum winch cable force for a tilt-up tower structure with a gin pole was considerably lower than the preliminary breaking force for a 40 mm winch cable, it was decided that the FE simulations were to be conducted again, with a winch cable of diameter 12 mm. This corresponded to a Grade 1960 6 × 7 with fibre core wire, which has a minimum breaking force of 93.7 kN as per AS3569 specification tables. The results of re-analysis, only considering the Tilt-Up Tower with a gin pole, are shown in Figure 5.5.

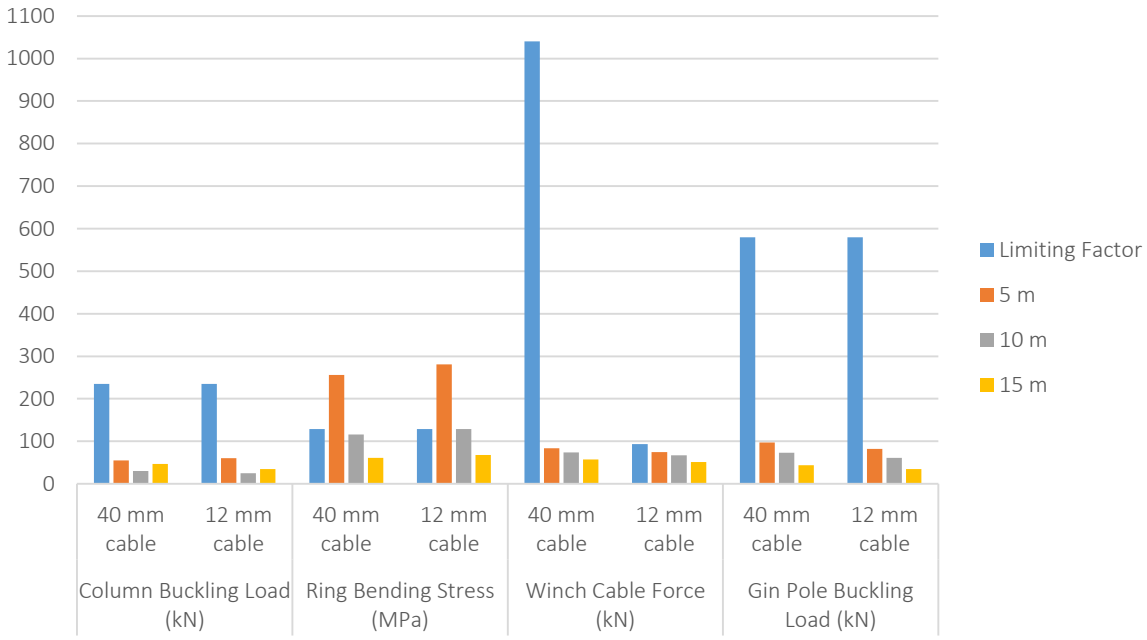

Figure 5.5: Tilt-Up Tower FE Simulation Results – Changing Winch Cable Diameter

When compared to the analysis results obtained using a 40 mm winch cable, it was evident that reducing the winch cable diameter to 12 mm has slightly reduce the winch cable force, whilst still being within the specification of limiting factor. It was also shown that all design criteria were within specification of the limiting factor as a result from changing the winch cable diameter, irrespective to any difference in results. The ring bending stress, however, increased slightly with decreasing cable diameter, and was shown to exceed the limiting factor for an

erection height of 5 m by 118%, as was the case when analysis was conducted with a 40 mm cable, which exceeded the limiting factor by 95%.

Further analysis was conducted, using a ring beam CHS with a greater wall thickness. A ring beam CHS of 323.9 × 12.7 mm, as opposed to a CHS of 323.9 × 9.5 mm was analysed, which resulted in a reduction in ring bending stress of 8% giving a ring bending stress of 261 MPa. This change was considered too insignificant for further analysis to be conducted by changing the ring beams CHS designation. A larger, thicker CHS may have eventually reduced the ring bending stress to within the design limiting factor specification, however larger, thicker CHS have a greater linear mass which would increase the load on both the columns and the winch cable throughout the erection procedure. Therefore, the feasibility of an alternative solution was briefly investigated, which included the addition of a secondary cable from the gin pole to the tower structure, as shown in Figure 5.6.

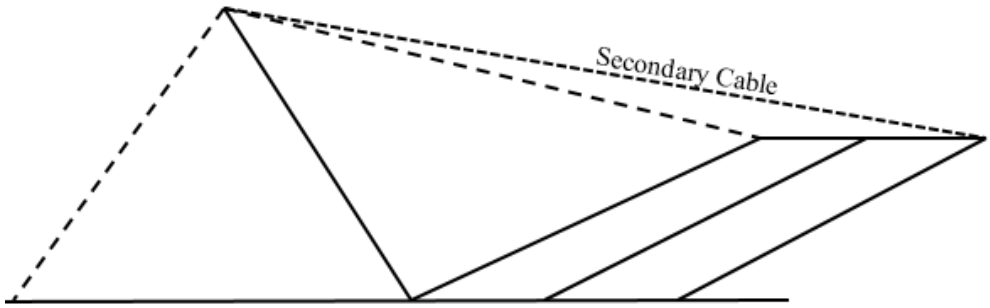

Figure 5.6: Schematic of Tilt-Up Tower Secondary Cable Attachment

The results from FE simulations conducted on the addition of a secondary cable from the gin pole to the tower structure are shown in Figure 5.7. Analysis was conducted using a winch and secondary cable diameter of 12 mm, and a ring beam CHS of 323.9 × 12.7 mm, for an erection height of 5 m. All other parameters remained unchanged.

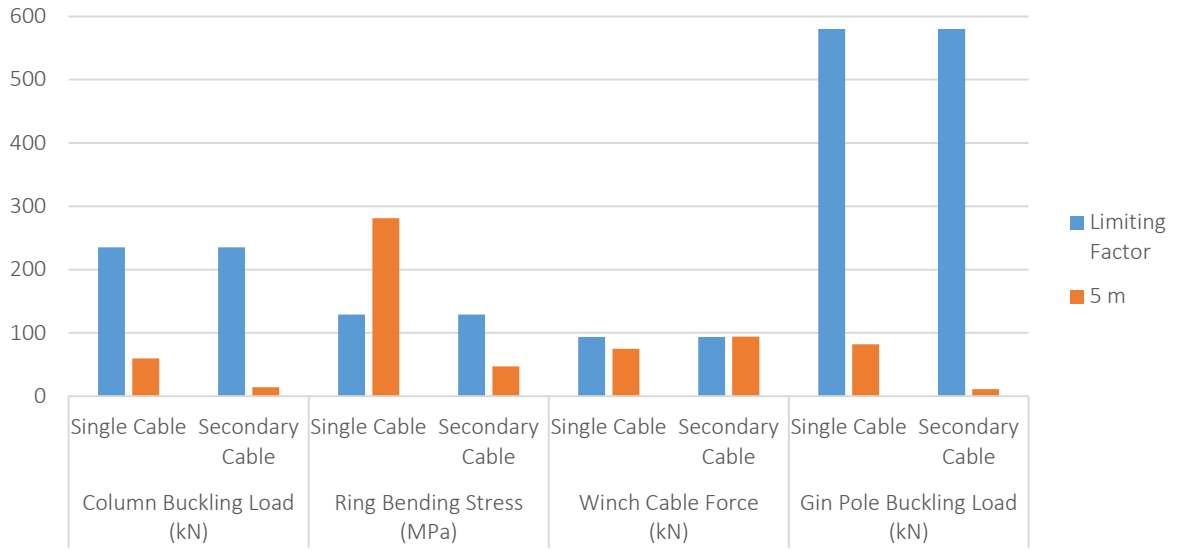

Figure 5.7: Tilt-Up Tower FE Simulation Results – Secondary Cable

The results show that the addition of a secondary cable significantly reduced the ring bending stress, and resulted in approximately an 83% reduction from 281 MPa to 47 MPa, which brought the ring bending stress within the limiting factor specification. The addition of the secondary cable also greatly reduced results for the column and gin pole buckling loads. The maximum cable force, which was found at the intersection point for the winch cable and secondary cable, was determined to be slightly greater than the specifications given by the limiting factor. Given the small difference between the maximum cable force and limiting factor, it could be assumed that by selecting the next largest cable diameter, 13 mm as per AS3569 specification tables, the design would meet the maximum permissible specification.

The only disadvantage with employing a secondary cable is the effectiveness at greater erection heights, and different gin pole parameters. If this cable were to act only as a support cable, independent of the winch cable, at erection heights where the gin pole heights is equal or less than that of the tower erection height, the secondary cable will interfere with the tower structure, and may lead to failure of either the tower or the cable. Without specific design of the secondary cable, a proposed solution would need to implement some sort of mechanism that disengages the cable from the tower structure when the gin pole heights is equal to the tower erection height.

5.4 Alternative Structural Geometries

The results from the analysis on alternative structural geometries, as outlined in Section 3.6.2, have been presented in the following section.

The analysis was initially conducted using a guy wire diameter of 12 mm, for a preliminary breaking force of 89 kN (calculated as described in Section 3.6.2, or refer to Appendix E), guy radius x_{guy} of 12 m as specified by Stapleton et al. [25], and consequently a θ_{guy} of 59°. The closest corresponding wire as per AS3569 tables was a 12 mm diameter Grade 1960 6 × 7 with fibre core, and has a minimum breaking force of 93.7 kN. It was assumed that the same guy wire parameters could be applied to the internally guyed structure. The results from the analysis on each alternative structure, for wind loading acting against rotation direction of member connections, are shown in Figure 5.8.

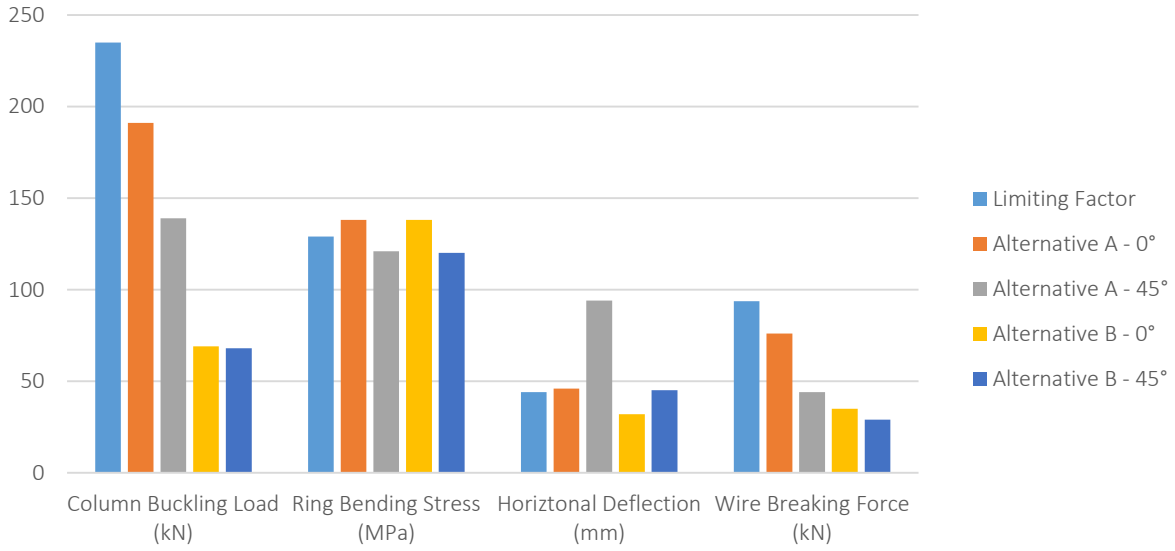

Figure 5.8: FE Simulation Results for Alternatives – Load Acting Against Connections

An additional analysis was conducted to observe the effects of loads applied across the rotation direction of member connections, and is shown in Figure 5.9. All parameters were unchanged. Loads were only applied at a wind orthogonal direction of 0° in this case, as the 45° direction would be the same as that for loading against rotation direction of member connections.

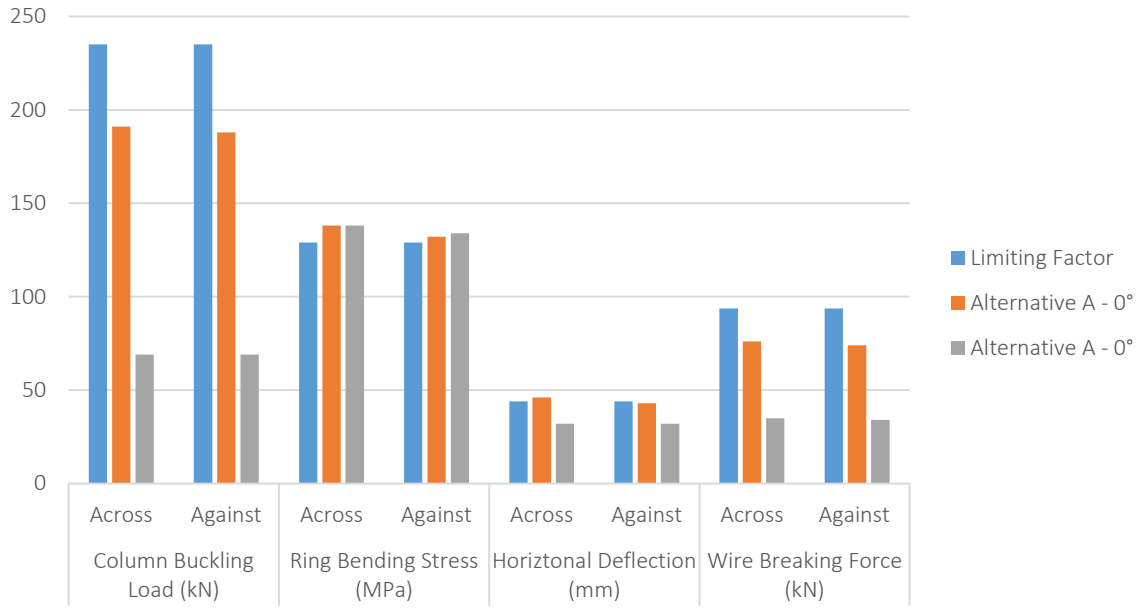

Figure 5.9: FE Simulation Results for Alternatives – Load Acting Across Connections

The results show that there was minimal difference between criteria if loads were applied against, or across the rotation direction of member connections, by comparing results for loading against and across connections.

The limiting factor was met in nearly all criteria. The results that showed the criteria with the greatest inability to meet the limiting factor, were that for the ring bending stress, as well as the maximum horizontal deflection, in Alternatives A and B. The greatest difference in ring bending stress, to that of the limiting factor, was 7%, and was considered manageable for further analysis to be conducted to produce a result within the limiting factor.

Hence, a ring beam section with greater wall thickness was selected, and the structure was re-analysed. Theoretically, increasing section wall thickness, increases the second moment of area, thus decreasing the bending stress in the beam. Figure 5.10 shows the results for analysis conducted on both structural geometries, using a ring beam CHS of 323.9 × 12.7 mm, as opposed to a CHS of 323.9 × 9.5 mm.

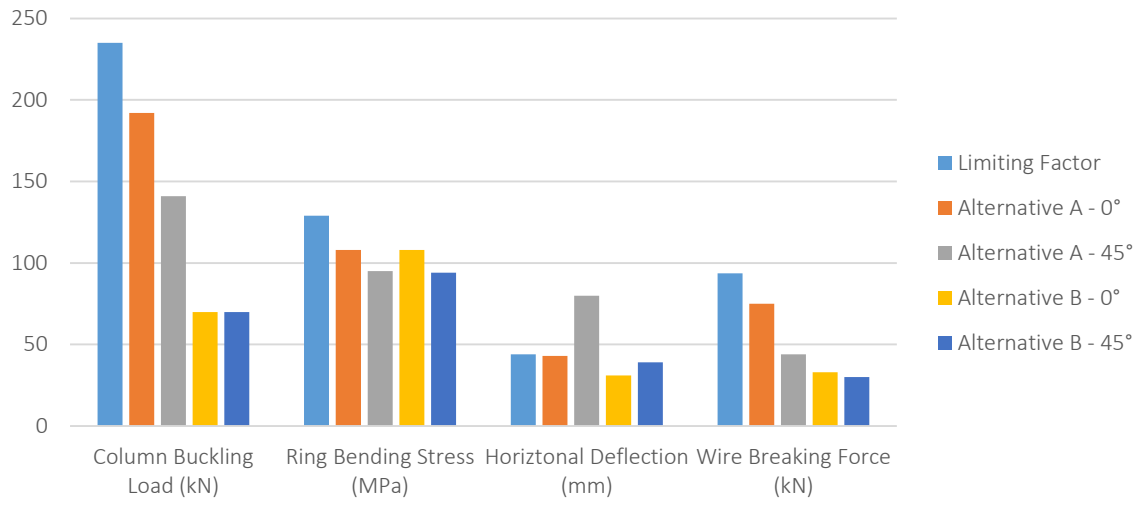

Figure 5.10: FE Simulation Results for Alternatives – Changing Ring Beam CHS

The results in Figure 5.10 show that increasing the ring beam section thickness reduced the ring bending stress for both alternative structural geometries, and for all wind orthogonal directions, and brought the results to within specification of the limiting factor. Increasing the ring beam section thickness also reduced the maximum horizontal deflection, however, loads applied at a wind orthogonal direction of 45° for Alternative A still exhibited a horizontal deflection greater than that of the limiting factor.

Theoretically, larger, and/or thicker columns will increase the second moment of area of the columns, which would increase the stiffness of the structure, thus decreasing the horizontal deflection. However, the column section would have to increase from a CHS of 273.1 × 6.4 mm to at least a CHS of 508 × 6.4 mm in order to meet the limiting factor. A column this size was considered impractical for the given application, as it could potentially affect the performance and feasibility of the tilt-up tower given the added weight associated with a larger section. Other changes that could be made to reduce the horizontal deflection include; increasing the guy wire radius x_{guy}, and increasing the guy wire diameter. To reduce the horizontal deflection, a large independent change can be made to a parameter without having to change another; however, such a large independent change renders the solution impractical for the given application within the aims of the design. Therefore, a combination of smaller changes in each parameter may offer a more practical solution.

Brief investigation and analysis resolved that Alternative A would meet the benchmark of design in all criteria if the parameters consisted of; ring beam CHS of 323.9 × 12.7 mm, column CHS of 323.9 × 9.5 mm, guy radius of 20 m, and a guy wire diameter of 22 mm of Grade 1570 6 × 7 with fibre core. The results from analysis under the new parameters are shown in Figure 5.11 in comparison to initial parameters.

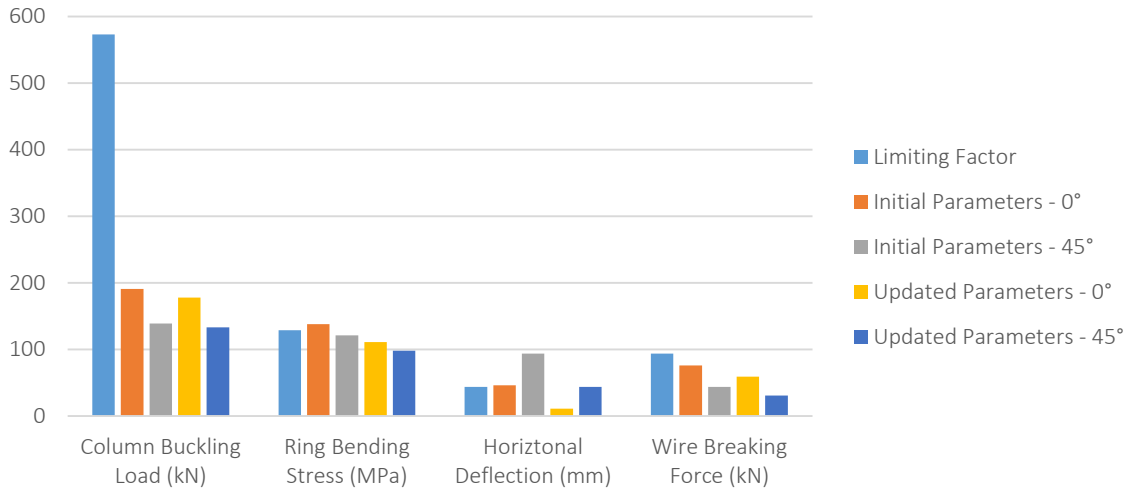

Figure 5.11: FE Simulation Results for Alternative A – Change in Parameters

Therefore, the analysis results in comparison to the benchmark of design for each alternative structural geometry can be summarised in Table 5.4 and Table 5.5 respectively.

Table 5.4: Summary of Analysis Results – Alternative A

Design Criteria	Limiting Factor	Wind Orthogonal Direction	
		0°	45°
Column Buckling Load (kN)	573	178	133
Ring Bending Stress (MPa)	129	111	98
Horizontal Deflection (mm)	44	11	44
Wire Breaking Force (kN)	252	59	31

The parameters that ensured Alternative B met the benchmark of design consisted of; ring beam CHS of 323.9 × 12.7 mm, column CHS of 273.1 × 6.4 mm, and a guy wire diameter of 12 mm of Grade 1960 6 × 7 with fibre core.

Table 5.5: Summary of Analysis Results – Alternative B

Design Criteria	Limiting Factor	Wind Orthogonal Direction	
		0°	45°
Column Buckling Load (kN)	235	70	70
Ring Bending Stress (MPa)	129	108	94
Horizontal Deflection (mm)	44	31	39
Wire Breaking Force (kN)	93.7	33	30

6 CONCLUSIONS

A comprehensive review of literature concerning the application of wind loading on cooling towers and similar structures, and tensile membrane structures, was conducted, and in accordance with relevant standards a methodology was formulated for the analysis of cooling towers within the scope of the thesis. It was concluded that cooling tower static structural loading would consist of a 3 kN/m membrane pretension load, and a 700 Pa wind pressure load, which equated to a 126 kN drag force.

A comparative study to validate the structural FEA results of a previous analysis on the QGECE Hybrid Cooling Tower was conducted. Results from the validation analysis concluded that there were significant oversights pertinent to the outcome of the previous analysis. Additional analysis was conducted accounting for these oversights and as a result, a benchmark of design was developed, and is summarised in Table 6.1.

Table 6.1: Benchmark of Design

Criteria	Limiting Factor
Column Buckling Load (kN)	573 (Alternative A) / 235 (Alternative B)
Ring Bending Stress (MPa)	129
Horizontal Deflection (mm)	44
Wire Breaking Force (kN)	≤ specified wire breaking force
Gin Pole Buckling Load (kN)	580

Investigation into alternative construction methods concluded that the use of a tilt-up tower would eliminate the need for large specific cranes for on-off lifts. Results from a feasibility analysis of tilt-up towers concluded that a tilt-up tower would only be feasible if a gin pole was used, and showed that with the aid of a gin pole a reduction in maximum structural axial force up to 75 times could be achieved as compared to a tilt-up tower without the aid of a gin pole. However, to meet the benchmark of design, the simplified structural geometry being analysed would need to be adjusted. The design parameters that met the benchmark of design are summarised in Table 6.2

Investigation into alternative structural geometries presented two solutions to accommodate a tilt-up tower, which simplified the existing structure by reducing the number of structural members in favour of guy wires. Extensive analysis was conducted on the two alternatives until a solution was established which met the benchmark of design, the design parameters for which are summarised, along with the design parameters for the tilt-up tower, in Table 6.2.

Figure 6.1, Figure 6.2, Figure 6.3, gives the schematic for each design solution configuration, the Tilt-Up Tower, Alternative A, and Alternative B respectively.

Table 6.2: Design Parameters for Proposed Solutions

Design Parameter	Tilt-Up Tower	Alternative A	Alternative B
Ring CHS	323.9 × 12.7 mm	323.9 × 12.7 mm	323.9 × 12.7 mm
Column CHS	273.1 × 6.4 mm	323.9 × 9.5 mm	273.1 × 6.4 mm
Guy Radius	-	20 m	-
Wire Designation - (Guy/Winch)	13 mm Grade 1960 6 × 7 with Fibre Core	22 mm Grade 1570 6 × 7 with Fibre Core	12 mm Grade 1960 6 × 7 with Fibre Core

Circular hollow sections, and steel wire rope specifications from relevant product and standards tables, for the given design parameters, are shown in Appendix F.

From the proposed solutions presented, the following significant conclusions were made towards the aims and objectives of the thesis:

- The Tilt-Up Tower will eliminate the need for specific cranes for one-off lifts, consequently reducing construction costs.
- The simplification of geometry, and reduction in the number of structural steel members in favour of guy wires in Alternatives A and B, thus further reduce construction costs, and consequently reducing the total installed cost per cooling tower.

While the Tilt-Up Tower and Alternative A improve on the existing QGECE Hybrid Cooling tower by reducing construction, capital, and manufacturing costs, whilst improving structural performance there are some trade-offs that would need to be considered for the solution to be completely viable. The Tilt-Up Tower makes a compromise on building footprint for reduced construction costs, however a larger area is only required for construction, the building footprint of the structure itself will be unchanged, depending on anchoring or bracing method. Alternative A compromises on building footprint in favour of reduced capital cost per tower, hence the feasibility of this solution would be circumstantial, depending on land area availability, and land lease costs. For these reasons, it can be concluded that the structure of Alternative B is the most suitable design solution for improving upon the existing QGECE Hybrid Cooling tower structural design.

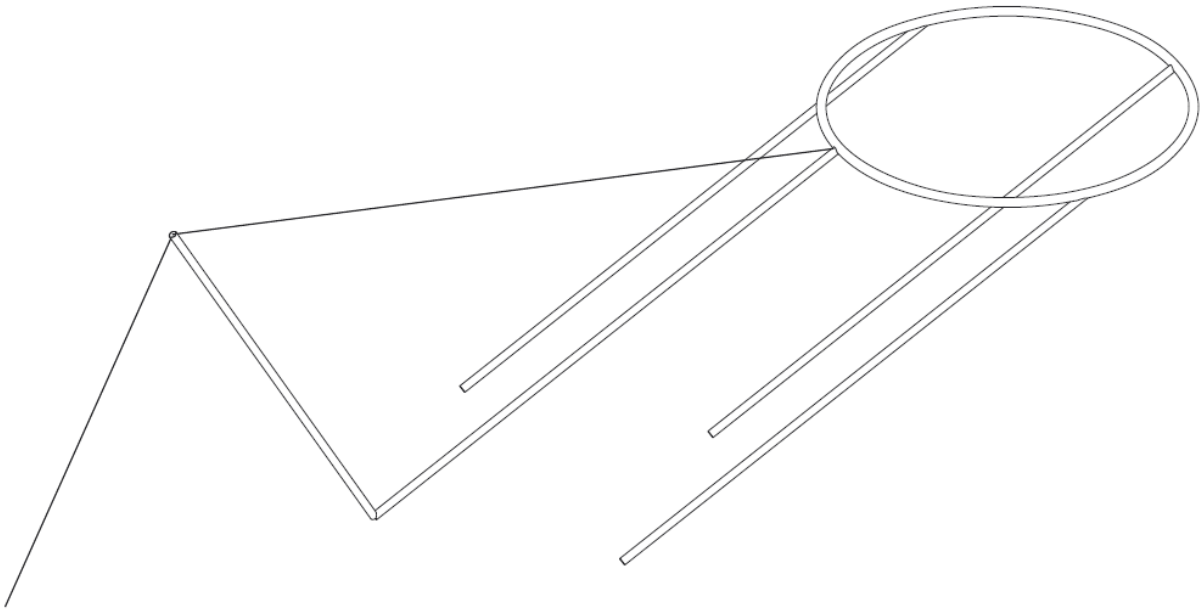

Figure 6.1: Design Solution – Tilt-Up Tower

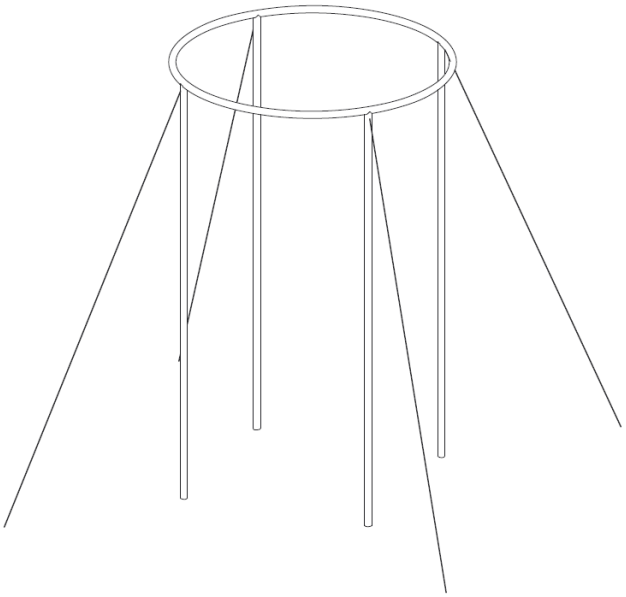

Figure 6.2: Design Solution – Alternative A

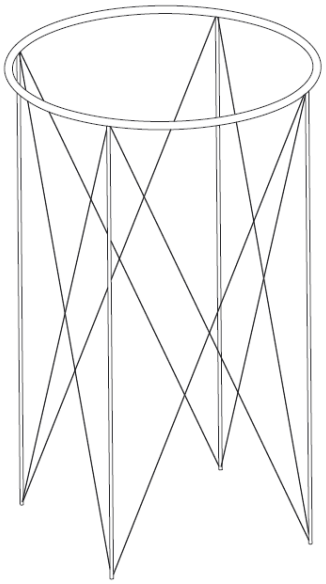

Figure 6.3: Design Solution – Alternative B

7 RECOMMENDATIONS

In summary, to improve upon the existing QGECE Hybrid Cooling Tower and reducing construction and manufacturing costs, and consequently reducing total installed cost per cooling tower, the following recommendations can be made:

- To reduce construction and cranage costs; implement the design proposal Tilt-Up Tower.
- To reduce manufacturing and total installed costs; implement design proposals Alternative A and/or Alternative B.

It is recommended that if a choice were to be made from the alternative structural geometries proposed, Alternative A and Alternative B, that Alternative B is the superior solution for the following reasons:

- Alternative B has a minimal installed building footprint.
- Alternative B uses optimally small diameter guy wires, which would reduce purchasing costs.
- Alternative B performs greater under loading conditions in terms of the benchmark of design.

To achieve a complete design solution further work will need to be conducted, including but not limited to the following;

- The detailed analysis and design of individual components to compensate for revised geometries such as pin connections and wire anchors.
- The detailed design of alternative anchoring for the PVC shell to compensate the removal of the bottom ring.

8 FURTHER CONSIDERATIONS

As mentioned in Section 7, to achieve a complete design solution additional analysis and design will need to be conducted. Some additional considerations will need to be made around the design itself before a completely feasible presentable solution can be offered.

A key component that was not considered in this thesis, was provisions for the mounting of heat exchangers inside the tower. Considerations would need to be made on how the heat exchangers are to be mounted inside the cooling tower, with particular focus on how the heat exchangers will be affected by loading on the tower structure. The stiffness of the tower at the heat exchanger mounting position would need to be considered, especially to minimise failure of damage to the heat exchanger as a result of adverse deformation. Also, depending on the total weight of the heat exchangers, the static loading of the tower structure attributing to the additional weight may need to be investigated for failure. Additional considerations may also include the assembly and installation of heat exchangers in association with the construction and erection of the structure as a whole.

Additional design work will need to be completed on connection components, in particular pin connections to accommodate the Tilt-Up Tower geometries. Anchor points for steel wire guy ropes will also need a detailed design, for both structural anchors and foundation anchors. Concrete footings for structural members, winch anchors, and guy wire anchors will also require detailed design analysis. Furthermore, because of the removal of the bottom ring beam in all presented solutions, the method of anchoring the bottom of the PVC membrane will need specific analysis. If concrete anchors are to be used for steel wire rope anchoring, and also for fixing the PVC membrane depending on fixing/anchoring method. The gin pole for the tilt-up tower may need a more thorough analysis to investigate the potential for optimised configurations. The connections of the gin pole will also need specific design, particularly for the connection from the base of the gin pole to the base of the tower column (options for either bolted or welded joints may need to be investigated), and the connection/sheave mechanism at the top of the gin pole to accommodate a running winch cable. The connection of the proposed second cable and disengaging mechanism at the top of gin pole, between the gin pole and tower, will also need a specific design investigation.

Further considerations would also need to be made about the assembly of tower peripheral components, such as the PVC membrane, and guy wires, prior to and during the erection procedure if the Tilt-Up Tower was to be used. The selection, and placement of a winch for use with the Tilt-Up Tower would also need to be factored in a final design solution.

9 REFERENCES

1. Barnes, D.F. *What is Rural Electrification: New Technologies and Old Definitions?* Energy for Development and Poverty Reduction, 2010.
2. Gwynn-Jones, S., et al., *Hybrid Natural Draft Dry Cooling Towers - An Enabling Technology for Remote Area Thermal Power Generation in Australia.* 2014.
3. Queensland Geothermal Centre of Excellence, *Annual Report 2014-2015*. 2015.
4. Universal Cranes, *Crane Specification: 25T Franna*. 2011.
5. Mohamed Shaharuddin, M.A., *Structural Analysis of Gatton Cooling Tower*. 2014, The University of Queensland: St. Lucia, Queensland.
6. Mehler Texnologies, *Engineered fabrics for extraordinary tensile architecture structures*. 2013.
7. Shellard, H.C., *COLLAPSE OF COOLING TOWERS IN A GALE, FERRYBRIDGE, 1 NOVEMBER 1965.* Weather, 1967. **22**(6): p. 232-240.
8. Murali, G., C.V. Vardhan, and B. Reddy, *Response of cooling towers to wind loads.* ARPN Journal of Engineering and Applied Sciences, 2012. **7**(1): p. 114-120.
9. Gaikwad, T.G., et al., *Effect of Wind Loading on Analysis of Natural Draught Hyperbolic Cooling Tower.* International Journal of Engineering and Advanced Technology, 2014. **4**(1): p. 34-39
10. Dryden, H.L. and G.C. Hill, *Wind pressure on circular cylinders and chimneys.* Bureau of Standards Journal of Research, 1930. **5**: p. 653-693.
11. Mollaert, M. and B. Forster, *European design guide for tensile surface structures.* Tensinet. Union Europea, 2004: p. 192-204.
12. Pun, P.K.F., *Analysis of a tension membrane HYPAR subjected to fluctuating wind loads*. 1993, The University of Queensland.
13. Takeda, F., T. Yoshino, and Y. Uematsu, *Design Wind Force Coefficients for Hyperbolic Paraboloid Free Roofs.* Journal of Physical Science and Application, 2014. **4**(1): p. 1-19.
14. Son, M.E., *The design and analysis of tension fabric structures*. 2007, Massachusetts Institute of Technology.
15. American Society of Civil Engineers, *ASCE/SEI 55-10: Tensile Membrane Structures*. 2010, American Society of Civil Engineers: Reston, VA.
16. Standards Australia, *Part 2: Wind actions*, in *AS1170.2:2011 Structural design actions*. 2011, SAI Global Limited: New South Wales, Australia.

17. Standards Australia, *AS4100:1998 Steel Structures*. 1998, SAI Global Limited: New South Wales, Australia.
18. Standards Australia, *AS1163:2016 Cold-formed Structural Steel Hollow Sections*. 2016, SAI Global Limited: New South Wales, Australia.
19. Standards Australia, *Product specification*, in *AS3569:2010 Steel wire rope*. 2010, SAI Global Limited: New South Wales, Australia.
20. Standards Australia, *Use, operation and maintenance*, in *AS2759:2004 Steel wire rope*. 2004, SAI Global Ltd.: New South Wales, Australia.
21. Standards Australia, *AS3600:2009 Concrete Structures*. 2009, SAI Global Limited: New South Wales, Australia.
22. American Institute of Steel Construction, *Crane Selection and Application*. 2006.
23. Han, S., et al., *A Framework for Crane Selection in Large-Scale Industrial Construction Projects*. 2013.
24. Armato, P., *When a Crane is Not Practical*, in *Hydraulic Cranes*, H.B. Inc., Editor. 2015.
25. Stapleton, G., et al., *Wind Systems*, in *Your Home: Australia's guide to Environment and Energy*. 2016, Commonwealth of Australia Department of the Environment and Energy,.
26. ANSYS Inc., *ANSYS Mechanical User's Guide*. 2013: Canonsburg, PA.
27. ANSYS Inc., *ANSYS DesignModeler User's Guide*. 2013: Canonsberg, PA.

APPENDIX A: RELATIONSHIP BETWEEN BUILDING ORTHOGONAL AXES AND WIND DIRECTIONS

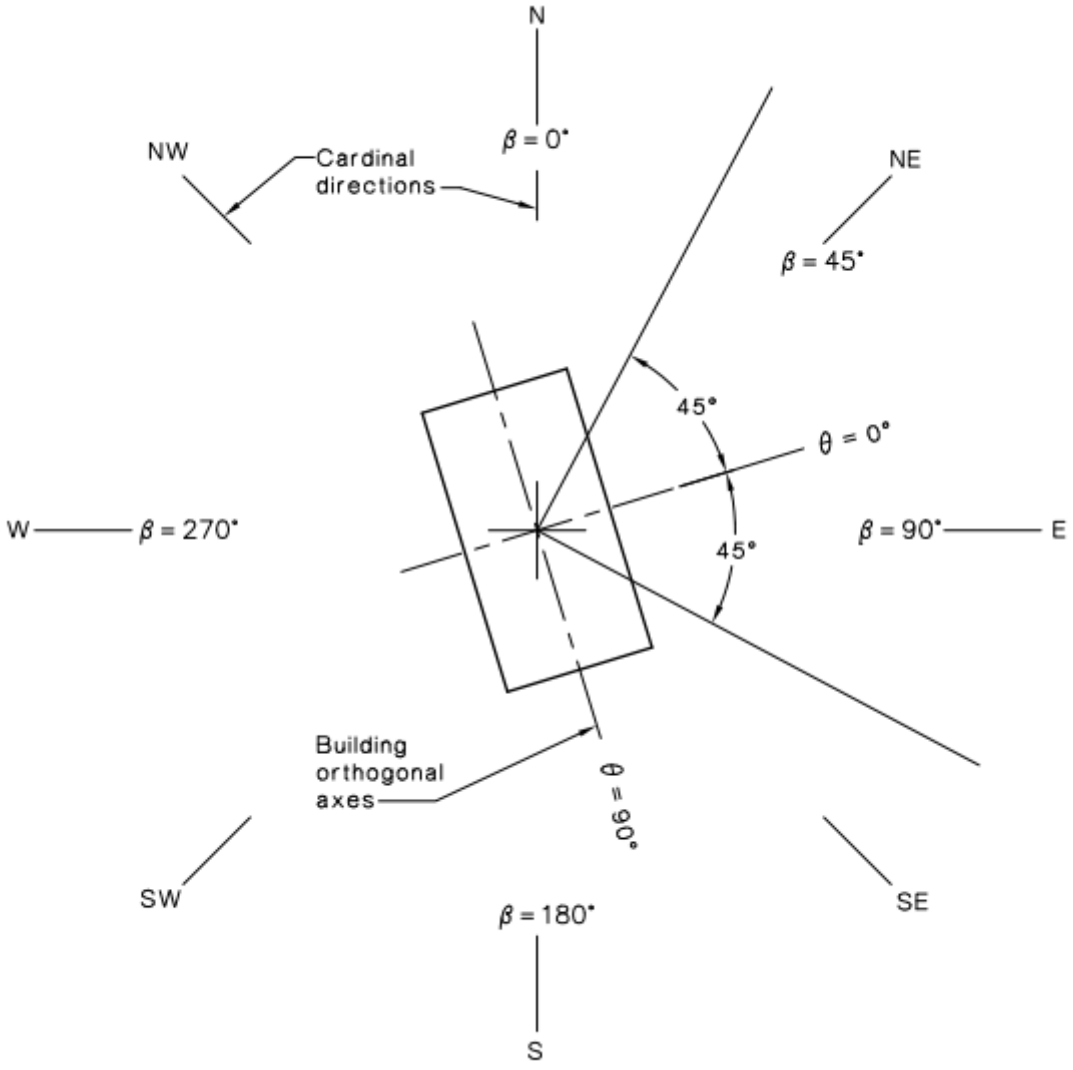

Figure A.1: Relationship Between Building Orthogonal Axes and Wind Directions [16]

APPENDIX B: APPLICATION OF WIND LOAD CALCULATIONS

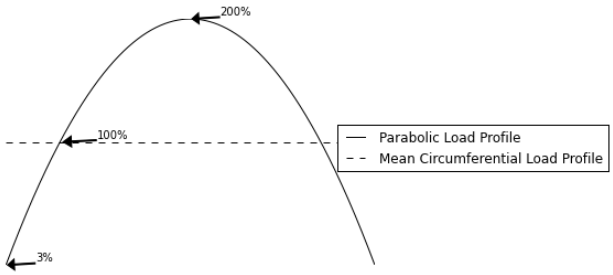

Figure B.1: Parabolic Load Distribution

The parabolic load profile was determined using the integral for a parabola proportional to the tower dimensions, given by Equation B.1, for a point along the width of the tower, to a sequential point given by a defined step size. Integration is iterated for the total width of the tower.

$$y_{parabolic} = \int_{x}^{x+i} -\frac{1}{6}(x-6)^2 + 6dx \quad \text{(B.1)}$$

$$y_{mean} = \int_{x}^{x+i} 3dx \quad \text{(B.2)}$$

The mean circumferencial load profile was determined using the integral for a unit rectangle, given by Equation B.2, for the width of the tower, integrating in incremental steps from zero, to a sequential point of the width of the tower, iterating for a number of steps that make up the width of the tower.. Being a rectangular profile the numerical solution would remain constant. The percentage load distribution was then calculated using Equation B.3.

$$\%\ Load\ Distribution = \left(\frac{y_{parabolic} - y_{mean}}{y_{mean}} + 1\right) \times 100 \quad \text{(B.3)}$$

Table B.1: Percent Load Distribution by Integral Points for Half Tower

Integral Points		Percent Load	Integral Points		Percent Load	Integral Points		Percent Load	Integral Points		Percent Load
0.0	0.1	3.31%	1.6	1.7	94.87%	3.1	3.2	154.87%	4.6	4.7	189.87%
0.1	0.2	9.87%	1.7	1.8	99.65%	3.2	3.3	157.98%	4.7	4.8	191.31%
0.2	0.3	16.31%	1.8	1.9	104.31%	3.3	3.4	160.98%	4.8	4.9	192.65%
0.3	0.4	22.65%	1.9	2.0	108.87%	3.4	3.5	163.87%	4.9	5.0	193.87%
0.4	0.5	28.87%	2.0	2.1	113.31%	3.5	3.6	166.65%	5.0	5.1	194.98%
0.5	0.6	34.98%	2.1	2.2	117.65%	3.6	3.7	169.31%	5.1	5.2	195.98%
0.6	0.7	40.98%	2.2	2.3	121.87%	3.7	3.8	171.87%	5.2	5.3	196.87%
0.7	0.8	46.87%	2.3	2.4	125.98%	3.8	3.9	174.31%	5.3	5.4	197.65%
0.8	0.9	52.65%	2.4	2.5	129.98%	3.9	4.0	176.65%	5.4	5.5	198.31%
0.9	1.0	58.31%	2.5	2.6	133.87%	4.0	4.1	178.87%	5.5	5.6	198.87%
1.0	1.1	63.87%	2.6	2.7	137.65%	4.1	4.2	180.98%	5.6	5.7	199.31%
1.1	1.2	69.31%	2.7	2.8	141.31%	4.2	4.3	182.98%	5.7	5.8	199.65%
1.2	1.3	74.65%	2.8	2.9	144.87%	4.3	4.4	184.87%	5.8	5.9	199.87%
1.3	1.4	79.87%	2.9	3.0	148.31%	4.4	4.5	186.65%	5.9	6.0	199.98%
1.4	1.5	84.98%	3.0	3.1	151.65%	4.5	4.6	188.31%	6.0	6.1	199.98%
1.5	1.6	89.98%									

Table B.2: Percent Load Distribution by Angle for Half Tower

Angle(°)	Percent Load	Angle(°)	Percent Load	Angle(°)	Percent Load	Angle(°)	Percent Load
90.00	3.31%	66.0	94.87%	43.5	154.87%	21.0	189.87%
88.5	9.87%	64.5	99.65%	42.0	157.98%	19.5	191.31%
87.0	16.31%	63.0	104.31%	40.5	160.98%	18.0	192.65%
85.5	22.65%	61.5	108.87%	39.0	163.87%	16.5	193.87%
84.0	28.87%	60.0	113.31%	37.5	166.65%	15.0	194.98%
82.5	34.98%	58.5	117.65%	36.0	169.31%	13.5	195.98%
81.0	40.98%	57.0	121.87%	34.5	171.87%	12.0	196.87%
79.5	46.87%	55.5	125.98%	33.0	174.31%	10.5	197.65%
78.0	52.65%	54.0	129.98%	31.5	176.65%	9.0	198.31%
76.5	58.31%	52.5	133.87%	30.0	178.87%	7.5	198.87%
75.0	63.87%	51.0	137.65%	28.5	180.98%	6.0	199.31%
73.5	69.31%	49.5	141.31%	27.0	182.98%	4.5	199.65%
72.0	74.65%	48.0	144.87%	25.5	184.87%	3.0	199.87%
70.5	79.87%	46.5	148.31%	24.0	186.65%	1.5	199.98%
69.0	84.98%	45.0	151.65%	22.5	188.31%	0.0	199.98%
67.5	89.98%						

APPENDIX C: TILT-UP TOWER CALCULATIONS

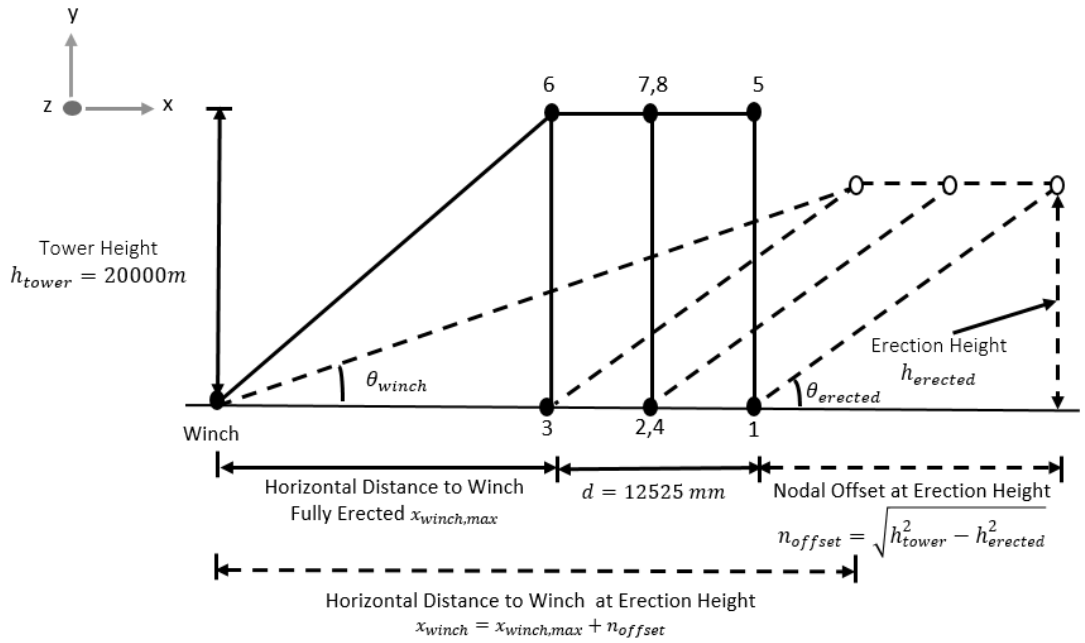

Figure C.1: Key Terms and Variables Used in Truss Analysis of Tilt-Up Tower

$$n_{offest} = \sqrt{h_{tower}^2 - h_{erected}^2} \quad (C.1)$$

$$\theta_{erected} = \tan^{-1}\left(\frac{h_{erected}}{n_{offset}}\right) \quad (C.2)$$

$$x_{winch} = x_{winch,max} + n_{offset} \quad (C.3)$$

$$\theta_{winch} = \tan^{-1}\left(\frac{h_{erected}}{x_{winch}}\right) \quad (C.4)$$

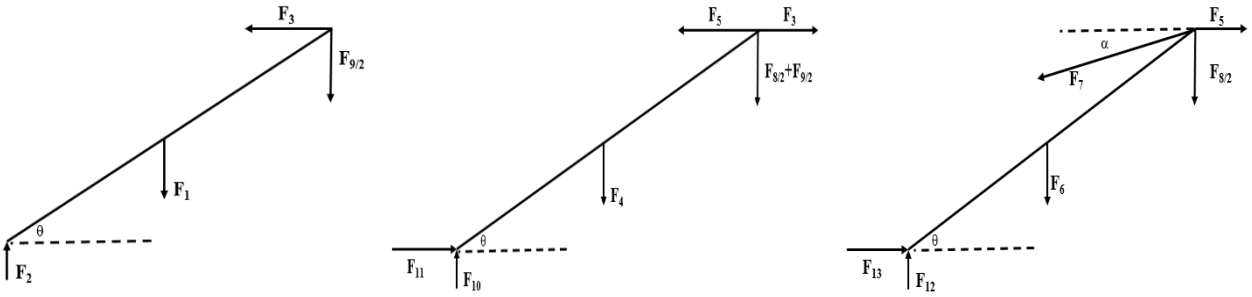

Figure C.2: Schematic of Tilt-Up Tower Nodal Forces

$$F_1 = F_4 = F_6 m_{column} g \quad (C.5)$$

$$\frac{F_8}{2} = \frac{F_9}{2} = \frac{1}{2}\frac{m_{ring} g}{2} \quad (C.6)$$

$$F_2 = F_1 + \frac{F_9}{2} \quad (C.7)$$

$$F_3 = \left[\frac{F_1}{2} + \frac{F_9}{2}\right]\frac{\cos\theta}{\sin\theta} \quad (C.8)$$

$$F_5 = F_{11} + F_3 \quad \text{(C.9)}$$

$$F_7 = \left[\frac{F_6}{2}\cos\theta + \frac{F_8}{2}\sin\theta + F_5\sin\theta\right]\frac{1}{\sin(\theta-\alpha)} \quad \text{(C.10)}$$

$$F_{10} = F_4 + \frac{F_8}{2} + \frac{F_9}{2} \quad \text{(C.11)}$$

$$F_{11} = \left[F_{10} - \frac{F_4}{2}\right]\frac{\cos\theta}{\sin\theta} \quad \text{(C.12)}$$

$$F_{12} = F_6 + \frac{F_8}{2} + F_7\sin\alpha \quad \text{(C.13)}$$

$$F_{13} = F_7\cos\alpha - F_5 \quad \text{(C.14)}$$

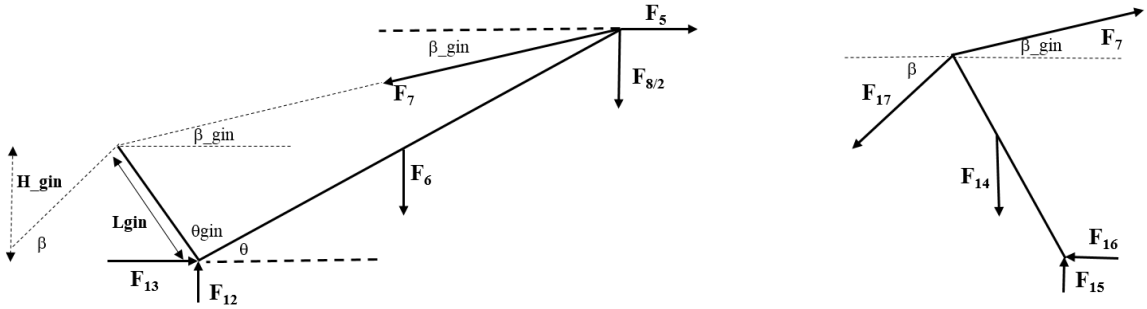

Figure C.3: Scehmatic of Gin Pole Nodal Forces

$$H_{gin} = L_{gin}\sin\left(180 - \theta_{gin} - \theta\right) \quad \text{(C.15)}$$

$$\beta = \tan^{-1}\left(\frac{H_{gin}}{x_{winch,max} - \sqrt{L_{gin}^2 - H_{gin}^2}}\right) \quad \text{(C.16)}$$

$$\beta_{gin} = \tan^{-1}\left(\frac{h_{erected} - H_{gin}}{n_{offset} - \sqrt{L_{gin}^2 - H_{gin}^2}}\right) \quad \text{(C.17)}$$

$$F_7 = \left[\frac{F_6}{2}\cos\theta + \frac{F_8}{2}\sin\theta + F_5\sin\theta\right]\frac{1}{\sin(\theta-\beta_{gin})} \quad \text{(C.18)}$$

$$F_{14} = m_{column}g \quad \text{(C.19)}$$

$$F_{15} = F_{14} + F_{17}\sin\beta - F_7\sin\beta_{gin} \quad \text{(C.20)}$$

$$F_{16} = F_{17}\cos\beta - F_7\sin\beta_{gin} \quad \text{(C.21)}$$

$$F_{17} = \begin{bmatrix} F_7\sin\left(180 - \theta - \theta_{gin} - \beta_{gin}\right) \\ -\frac{F_{14}}{2}\cos\left(180 - \theta - \theta_{gin}\right) \end{bmatrix}\frac{1}{\sin(180-\theta-\theta_{gin})} \quad \text{(C.22)}$$

APPENDIX D: BUCKLING LOAD CALCULATIONS

$$N_{om} = \frac{\pi^2 EI}{(k_e l)^2} \quad \text{(D.1)}$$

where

N_{om} = elastic buckling load of a member

E = Young's modulus

I = cross-sectional moment of area of a member

k_e = member effective length factor

l = member length

	Braced member			Sway member		
Buckled shape						
Effective length factor (k_e)	0.7	0.85	1.0	1.2	2.2	2.2
Symbols for end restraint conditions	= Rotation fixed, translation fixed			= Rotation fixed, translation free		
	= Rotation free, translation fixed			= Rotation free, translation free		

Design buckling load calculated for the original structure with CHS 273.1 × 6.4 mm, and fixed-fixed braced end constraints:

$$N_{om,original\ columns} = \frac{\pi^2 \times 200 \times 10^9 \times \left(\pi/4\,(r_o^4 - r_i^4)\right)}{(0.7 \times 20)^2} = 480\ kN$$

Design buckling load calculated for the alternative structures with CHS 273.1 × 6.4 mm, and pin-pin braced end conditions:

$$N_{om,new\ columns} = \frac{\pi^2 \times 200 \times 10^9 \times \left(\pi/4\,(r_o^4 - r_i^4)\right)}{(1.0 \times 20)^2} = 235\ kN$$

Design buckling load calculated for the alternative structures with CHS 323.9 × 9.5 mm, and pin-pin braced end conditions:

$$= 573\ kN$$

Design buckling load calculated for the gin pole with CHS 273.1 × 6.4 mm, and fixed-pin braced end conditions:

$$N_{om,gin} = \frac{\pi^2 \times 200 \times 10^9 \times \left(\pi/4\,(r_o^4 - r_i^4)\right)}{(0.85 \times 20)^2} = 580\ kN$$

APPENDIX E: PRELIMINARY WIRE BREAKING FORCE CALCULATIONS

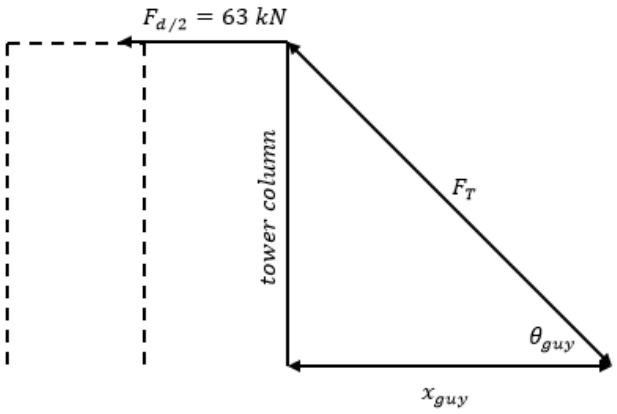

$$\theta_{guy} = \tan^{-1}\left(\frac{h_{tower}}{x_{guy}}\right) \quad \text{(E.1)}$$

$$F_T = \frac{F_{d/2}}{\cos(\theta_{guy})} \quad \text{(E.2)}$$

APPENDIX F: DESIGN PARAMETER DESIGNATION SPECIFICATIONS

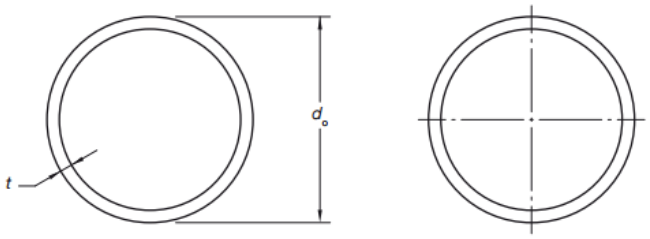

1			2	3	4	5	6	7	8	9	10	11	12
Designation			Mass per unit length	External surface area		Ratio	Gross area of cross-section	About any axis				Torsion constant	Torsion modulus
Outside diameter		Thickness		Per unit length	Per unit mass			Second moment of area	Elastic section modulus	Plastic section modulus	Radius of gyration		
d_o	×	t	m	A_{EL}	A_{EM}	$\frac{d_o}{t}$	A_g	I	Z	S	r	J	C
mm	×	mm	kg/m	m^2/m	m^2/t		mm^2	$10^6\ mm^4$	$10^3\ mm^3$	$10^3\ mm^3$	mm	$10^6\ mm^4$	$10^3\ mm^3$
457.0	×	12.7 CHS	139	1.44	10.3	36.0	17700	438	1920	2510	157	876	3830
457.0	×	9.5 CHS	105	1.44	13.7	48.1	13400	334	1460	1900	158	669	2930
457.0	×	6.4 CHS	71.1	1.44	20.2	71.4	9060	230	1010	1300	159	460	2010
406.4	×	12.7 CHS	123	1.28	10.4	32.0	15700	305	1500	1970	139	609	3000
406.4	×	9.5 CHS	93.0	1.28	13.7	42.8	11800	233	1150	1500	140	467	2300
406.4	×	6.4 CHS							792	1020	141	322	1580
355.6	×	12.7 CHS							1130	1490	121	403	2260
355.6	×	9.5 CHS	81.1	1.12	13.8	37.4	10300	155	871	1140	122	310	1740
355.6	×	6.4 CHS	55.1	1.12	20.3	55.6	7020	107	602	781	123	214	1200
323.9	×	2.7 CHS	97.5	1.02	10.4	25.5	12400	151	930	1230	110	301	1860
323.9	×	9.5 CHS	73.7	1.02	13.8	34.1	9380	116	717	939	111	232	1430
323.9	×	6.4 CHS	50.1	1.02	20.3	50.6	6380	80.5	497	645	112	161	994

Note Typo in Standard: Should read 12.7

1			2	3	4	5	6	7	8	9	10	11	12
Designation			Mass per unit length	External surface area		Ratio	Gross area of cross-section	About any axis				Torsion constant	Torsion modulus
Outside diameter		Thickness		Per unit length	Per unit mass			Second moment of area	Elastic section modulus	Plastic section modulus	Radius of gyration		
d_o	×	t	m	A_{EL}	A_{EM}	$\frac{d_o}{t}$	A_g	I	Z	S	r	J	C
mm	×	mm	kg/m	m^2/m	m^2/t		mm^2	$10^6\ mm^4$	$10^3\ mm^3$	$10^3\ mm^3$	mm	$10^6\ mm^4$	$10^3\ mm^3$
273.1	×	6.4 CHS	42.1	0.858	20.4	42.7	5360	47.7	349	455	94.3	95.4	699

Figure F.1: Circular Hollow Section Specifications

TABLE C1

CLASS 6 × 7 WITH FIBRE CORE

Typical cross-section		Typical construction			
		Rope construction	Strand construction	Outer wires	
				Total	Per strand
		6 × 7–FC	1–6	36	6
Nominal rope diameter *(d)* mm	Approximate nominal length mass kg/100 m	Minimum breaking force			
		Grade 1570 kN	Grade 1770 kN	Grade 1960 kN	
2	1.3	2.1	—	—	
3	3.1	4.7	—	—	
3.5	4.2	6.4	—	—	
4	5.5	8.4	—	—	
5	8.6	13.1	—	—	
6	12.4	18.8	21.2	23.4	
7	16.9	19.3	21.8	31.9	
8	22.1	33.4	37.6	41.6	
9	27.6	42.2	47.6	52.7	
10	34.5	52.2	58.8	65.1	
11	41.7	63.1	71.1	78.7	
12	49.7	75.0	84.6	93.7	
13	58.3	88.1	99.3	110	
14	67.6	102	115	128	
16	88.3	133	150	167	
18	112	169	190	211	
19	125	188	212	235	
20	138	208	235	260	
22	167	252	284	315	
24	199	—	338	375	
26	233	—	397	440	
28	270	—	461	510	
32	353	—	602	666	
35	423	—	720	797	
35	423	—	720	797	
36	447	—	762	843	
38	498	—	849	940	
40	552	—	940	1040	

Figure F.2 Steel Wire Rope Specifications